Green Chemistry

TUTORIAL REVIEW

View Article Online
View Journal | View Issue

Open Access Article. Published on 20 May 2022. Downloaded on 14/09/2025 22:14:34.
This article is licensed under a Creative Commons Attribution-NonCommercial 3.0 Unported Licence.

Check for updates

Cite this: *Green Chem.*, 2022, **24**, 4328

Semi-continuous and continuous processes for enantiomeric separation†

Marina Ciriani, *[a,b] Rudi Oliveira [a] and Carlos A. M. Afonso [b]

Received 5th October 2021,
Accepted 8th February 2022

DOI: 10.1039/d1gc03668h

rsc.li/greenchem

Chiral resolution is an operation of great interest and increasing importance for the scientific community and industry. There are two approaches to provide enantiomerically pure compounds: by asymmetric synthesis of just one of the enantiomers or by resolution of racemates consisting of separating a mixture of both enantiomers. In the past years, extraordinary progress has been achieved in continuous enantiomeric separation, implementing more efficient procedures, and contributing to developing greener and more sustainable separation processes. This review article covers the main topics and applications of semi-continuous and continuous chiral separation focusing, in particular, on preferential crystallization, membrane separations, and continuous chromatography. It also offers an authors' perspective on potential future directions in the field.

1. Introduction

Molecular chirality was discovered by Louis Pasteur, in 1848.[1] He found out that some molecules could exist as two non-superimposable-mirror image forms. Today, we know this type of molecule as enantiomers. Enantiomers are stereoisomers molecules with identical atomic constitution but have a non-superimposable mirror image, in other words, their three-dimensional arrangement of atoms is different. They have identical physical properties except for optical rotatory.[2,3] The

[a]*Hovione Farmaciência, S.A. Sete Casas, 2674-506 Loures, Portugal. E-mail: marinaciriani@tecnico.ulisboa.pt, rsoliveira@hovione.com, carlosafonso@ff.ulisboa.pt*

[b]*Research Institute for Medicines (iMed.ULisboa), Faculty of Pharmacy, Universidade de Lisboa, Avenida Professor Gama Pinto, 1649-003 Lisbon, Portugal*

†The authors picked the best-case scenario reported in each article to present here.

Marina Ciriani

Marina Ciriani is currently a Scale-up Design Scientist at Hovione Farmaciência S.A and, since 2016, she has been working on the process development of sensitive active pharmaceutical compounds using continuous flow technologies and modeling. She obtained a Bachelor of Science in Chemical Engineering and a Master of Science in Pharmaceutical Engineering. She is also pursuing her Ph.D. in the Medicinal Chemistry Department of the Faculty of Pharmacy at the University of Lisbon in partnership with Hovione Farmaciência, S.A.

Rudi Oliveira

Rudi Oliveira is currently a Senior Scientist at Hovione FarmaCiência SA and an Invited Auxiliary Lecturer at the University of Lisbon. In 2014, he received his Ph.D. in Medicinal Chemistry under the supervision of Professors Francisca Lopes and Rui Moreira from the University of Lisbon (PT) and Professor Paul M. O'Neill from the University of Liverpool (UK). After a PostDoc in Chemical Biology (2015), he joined Hovione FarmaCiência SA to participate in the build-up of a Continuous Manufacturing group. Since then, he has worked in the development and scale-up of chemical processes both in batch and continuous. His research interests are currently focused on continuous unit operations and modern scale-up tools.

This journal is © The Royal Society of Chemistry 2022

Open Access Article. Published on 20 May 2022. Downloaded on 14/09/2025 22:14:34.
This article is licensed under a Creative Commons Attribution-NonCommercial 3.0 Unported Licence.

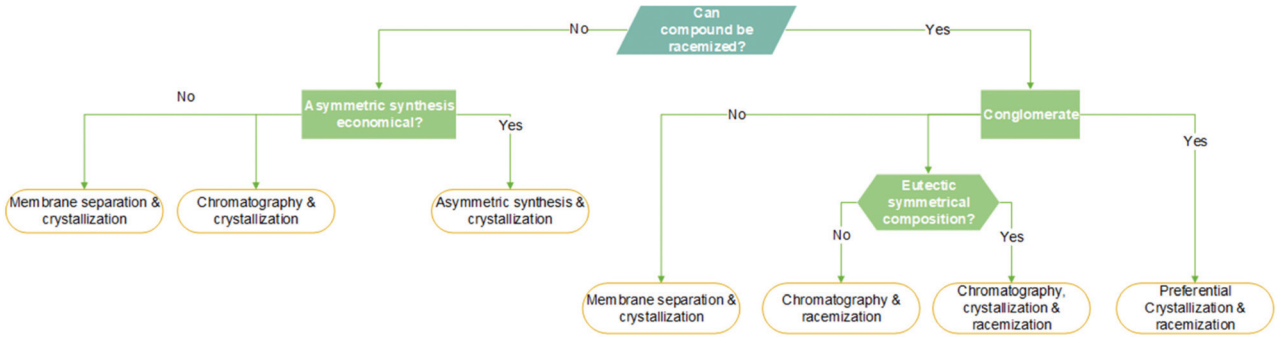

Fig. 1 Decision tree based on qualitative criteria for the selection of feasible unit operations for the obtention of pure enantiomers. Adapted from ref. 11 and 18.

classical notations for enantiomers are D or L (commonly used for amino acids and sugars), *R* or *S*, and/or (+) or (−) which relates the ordering of the ligands to the chiral center.[4]

Nowadays, it is known that chirality influences the biological and physical properties of molecules. The Global Chiral Chemicals Market size is estimated to be USD 57.79 billion in 2019 and is predicted to reach USD 150.64 billion by 2030 with a compound annual growth rate of 9.1% from 2020–2030.[5]

Increasing government focus on pharmaceutical manufacturing and rising investment by the manufacturers in emerging economies are the major factors propelling the market growth. Today, more than 80% of the drugs that are manufactured contain a chiral center due to the approval by FDA as safe ingredients.[5] The growing demand for targeted pharmaceutical offerings and eco-friendly agrochemical products continues to be a key factor driving growth.[6]

Evidence exists that frequently only one enantiomer of a chiral active pharmaceutical ingredient provides the desired pharmacokinetic, physiological, and toxicological properties.[4,5] Also, regulatory authorities require a scientific-based justification for any proposal to market a racemic mixture.[7–10] Thus, producing pure enantiomers is key for the pharmaceutical industry.[11] Chiral active pharmaceutical ingredients available in the market are for example: (*S*)-propanolol, (*S*)-naproxen, levosalbutamol, flavopiridol, *etc*. And, some racemic drugs also available are ibuprofen, salbutamol (Ventilan™), fluoxetine (Prozac™), *etc*.[12,13]

There are two approaches to provide enantiomerically pure compounds: by asymmetric synthesis of just one enantiomer (chemical or chemoenzymatic) or by resolution of racemic mixtures. The attractive option in terms of reagent consumption would be asymmetric synthesis that makes use of fermentation, chiral source synthesis (chiral pools), and asymmetric catalysis.[14] Significant progress was achieved in this field in the last years but the procedures are still limited in scope and do not provide directly the required purity.[15] Consequently, it is crucial developing new processes to separate enantiomers. The two major operations for chiral resolution are chiral chromatography and crystallization.[16] Different types of chromatography exist for enantiomeric resolution namely, high-performance liquid chromatography, simulated moving bed chromatography, supercritical fluid chromatography, ionic-liquid assisted ligand exchange chromatography,[17] and others. Most often, crystallization is the chosen operation because it is widely applicable, scalable, and cost-effective.[11]

An article guideline for an efficient selection of promising process operations for enantiomeric separation can be found in the literature,[18] and it is based on experience gained with a large number of industrial case studies. Fig. 1 can be used to identify feasible unit operations for each case of enantiomeric separation based on physicochemical properties available in an early stage of development. It must be known if racemization is possible, if conglomerate is present and which is the eutectic composition of the chiral system. As a result of this knowledge, it can be identified possible strategies to perform the chiral resolution. Although asymmetric synthesis is not approached in this review, if racemization is unachievable, a stereoselective synthesis might be performed if economically

Carlos A. M. Afonso

Carlos A. M. Afonso is currently Full Professor at Faculty of Pharmacy, University of Lisbon. He received his PhD in 1990 under supervision of Professor C. D. Maycock, subsequently became Assistant Professor at New University of Lisbon and Associate Professor at Instituto Superior Técnico in Lisbon (2004–2010), and took a post-doctoral fellow (1990) at Imperial College of Science Technology and Medicine (W.B. Motherwell) and sabbatical leave (1997/1998) at University of Bath, UK (Jonathan Williams) and at the University of Toronto (Robert Batey). His current research is mainly focused on synthetic methodologies, more sustainable chemistry, synthetic valorisation of national natural resources and synthesis of bioactive molecules.

Open Access Article. Published on 20 May 2022. Downloaded on 14/09/2025 22:14:34.
This article is licensed under a Creative Commons Attribution-NonCommercial 3.0 Unported Licence.

attractive. The other options would be chromatography, crystallization, membrane separation, or a combination thereof. If racemization is possible, it should be applied in sequence with a resolution operation feasible for: (1) conglomerate systems that would be preferential crystallization or; (2) the compound-forming system with two eutectics at symmetrical compositions that would be chromatography, crystallization, and membrane separation.

1.1. Continuous processes and Green Chemistry

The field of Green Chemistry demonstrates how process scientists and chemists might develop products and processes that can be profitable and at the same time good for human health and the environment.[19] Throughout in this review, we will address the pertinent Green Chemistry principles by the references listed in Table 1.

Table 1 The 12 principles of green chemistry. Based on ref. 19

Reference	Green chemistry principle
P1	Prevention
P2	Atom economy
P3	Less hazardous chemical syntheses
P4	Designing safer chemicals
P5	Safer solvents and auxiliaries
P6	Design for energy efficiency
P7	Use of renewable feedstocks
P8	Reduce derivatives
P9	Catalysis
P10	Design for degradation
P11	Real-time analysis for pollution prevention
P12	Inherently safer chemistry for accident prevention

Continuous crystallization (chapter 2) can offer considerable advantages such as elimination of batch to batch variability, particle size control, scalability of the process, reduced capital expenditure (CapEx) and operational expenditure (OpEx) along with the more efficient use of energy and materials (**P6**).[20]

Membrane separation (chapter 3) is a robust and green unit operation for the purification and separation of desired compounds streams that takes a shift towards a continuous methodology and presents minimal energy requirements (**P1**, **P6**).[20]

The use of supercritical fluids, namely supercritical carbon dioxide ($scCO_2$) is an interesting approach for continuous processes since they are inaccessible without high-pressure environments. The application of supercritical fluids in a flow system offers numerous advantages over batch vessels and has proven to be one valuable alternative to traditional solvents.[19] The operations may be performed on a small scale, improving safety and reducing the amount of material required (**P1**, **P5**).[21] Examples using $scCO_2$ for enantiomeric separation are given in chapters 4 and 5 of this review.

The bibliography of this work was obtained through the SciFinder database of the American Chemical Society and the Web of Knowledge database of the Clarivate Analytics. No restriction to publication date was applied. The search was done in the period between January and December of 2021.

2. Crystallization

Crystallization is a solid–liquid separation and purification process very commonly used in the fine chemical, pharmaceutical, agrochemical, and food industries. More than 90% of active pharmaceutical ingredients (API) are isolated as crystalline products.[22,23] During crystallization, parameters such as morphology and size distribution must be strictly controlled due to their great influence on the quality, physical and chemical properties of the resulting product. It can also affect downstream operations such as the time of drying, milling, and filtration.[34] A tutorial review on how to rationally conduct a crystallization of a stable or a metastable phase in solution is given by Coquerel.[24] Vetter *et al.*[25] described a methodology that allows finding regions of attainable particle sizes in batch and continuous crystallization processes.

The obtention of enantiopure chemicals can be achieved by using crystallization procedures such as the classical resolution, preferential crystallization, optically active solvent methods, and attrition-enhanced deracemization (Viedma Ripening).[11] In 1853, Pasteur developed the classical and most known method for enantiomers purification, the Pasteurian resolution.[26] He performed the resolution of tartaric acid using chiral quinuclidine bases. The method is based on adding a chiral agent to the racemic solution, breaking the thermodynamic symmetry of the enantiomers by forming diastereomeric compounds in the form of complexes or salts.[15,27] Diastereomers have different physicochemical properties, for example, solubility, which allow the separation to be achieved. This is a feasible approach used in large-scale processes for enantiomers resolution. A synthetic intermediate of the anticancer drug flavopiridol, and (*S*)-naproxen an anti-inflammatory drug are produced on an industrial-scale using the Pasteurian resolution.[28,29] However, this classical technique presents some disadvantages. The chiral agent must be added in stoichiometric amounts (going against **P2**, **P8** and **P9**), must be inexpensive, and be available in the market with high chemical and optical purities.[15] Moreover, there is no rule to find an optimal chiral resolving agent. Numerous candidates must be experimentally tested to discover the chiral agent that changes considerably the solubility between the forming diastereomers allowing the isolation of the desired one by crystallization. Finally, a noncovalent bond between the chiral agent and the pair of enantiomers is required for an easy recovery of the target enantiomer following crystallization.

In a preferential crystallization process feasible only for conglomerate-forming systems, by seeding of a racemic or enantiomerically enriched solution with crystals of the preferred pure enantiomer, control over the crystallizing enantiomer is obtained.[30] In 1969, Sato *et al.*[31] described a preferential crystallization batch procedure to prepare 95% pure (D)-lysine-3,5-dinitrobenzoate from a racemic mixture. Also, kinetically controlled crystallization of a racemic conglomerate is possible in the presence of chiral polymers at a certain temperature. The polymer inhibits the precipitation of the undesired enantiomer, collecting the desired one by filtration (against **P2**).

 This journal is © The Royal Society of Chemistry 2022

Open Access Article. Published on 20 May 2022. Downloaded on 14/09/2025 22:14:34.
This article is licensed under a Creative Commons Attribution-NonCommercial 3.0 Unported Licence.

In 2005, Viedma described an abrasion-grinding method for total symmetry breaking and obtention of complete chiral purity (**P1** and **P2**).[32] The author demonstrated the development of a homochiral solid phase for the inorganic compound $NaClO_3$, initially present as a racemic mixture of two enantiomorphic solid phases in equilibrium with the achiral aqueous phase. A population balance model was described by Iggland *et al.*[33] to explain the experimental behavior observed by Viedma. Later, this new symmetry-breaking technique was used for the *enantio*-enrichment of racemic mixtures of aminoacids compounds such as aspartic acid.[34,35] In 2019, Baglai *et al.*[36] described a procedure to synthesize a precursor of Levetiracetam and Brivaracetam using Viedma Ripening approach. A review covering the asymmetric crystallization process emphasizing Viedma approach is given by Rutjes *et al.*[37]

In recent years, improved processes variants involving either preferential crystallization, Viedma ripening, or combinations thereof have been reported in the literature in batch and continuous mode. In this review chapter, we will discuss the remarkable improvements for continuous preferential crystallization to obtain enantiopure compounds.

2.1. Preferential crystallization

Preferential Crystallization (PC) is a productive and cost-effective method to obtain crystals of a single enantiomer from a racemic solution.[27] To use this methodology, the chiral system must occur as a conglomerate meaning that the enantiomers crystallize as separate enantiopure crystals. Only 10% of the racemic mixtures belong to the conglomerate forming group.[38] Phase diagram screenings of enantiomer mixtures in a solution can give important indications on the possibility of chiral resolution through crystallization.[39]

The process is carried out in the metastable zone determined by phase diagrams analysis. In this specific zone, it is possible to preferentially develop crystals of the desired enantiomer with high yields and productivities through a seeded process. The seeding will avoid the nucleation of counter-enantiomer due to the initial homochiral surface area.[16] To obtain high purity and yields, the process must be stopped before the undesired counter enantiomer crystallizes.[38] Using preferential crystallization to obtain pure enantiomeric compounds can be labor-intensive and require careful monitoring and control of process parameters.

There are several techniques and operation set-ups that can be used with single or coupled crystallizers of different types. Seeded Isothermal Preferential Crystallization is a preferential crystallization technique where the pure enantiomer is crystallized by seeding a supersaturated solution at a constant temperature. An isothermal batch crystallization process should be stopped before the nucleation of crystals of the undesired enantiomer occurs so that only pure crystals of the desired enantiomer can be collected. Petruševska-Seebach *et al.*[40] described the resolution of (L)-asparagine in water using simple isothermal batch preferential crystallization. A precise stopping of the crystallization and rapid filtration of the product crystals is a very high-risk operation, thus preferential crystallization processes can be carried out in a polythermal method.[16]

Auto-Seeded Polythermal Programmed Preferential Crystallization (AS3PC) is one approach to perform preferential crystallization developed by Coquerel *et al.*[41] where the pure enantiomer is crystallized by application of a controlled cooling until the obtention of a saturated solution. Some examples using this method are the preferential crystallization of 4-carboxyphenylglycine,[42] omeprazole,[43] (±)-5-(4-bromophenyl)-5-methylhydantoin,[44] baclofenium hydrogenomaleate[45] and (D/L)-threonine.[46] Stirring may also be an important parameter to monitor and control during preferential crystallization as described for the resolution of 5-ethyl-5-methylhydantoin.[47,48]

From batch to continuous crystallization. In industry, the obtention of crystal shape molecules traditionally is done by discontinuous or batch crystallization due to the simplicity of crystallization equipment, and manual operation.[49,50] Although, it presents some shortcomings such as scale-up challenges, high costs, and batch-to-batch variability.[22] Over the last two decades, the continuous mode has gained the interest of industry and academia due to its many advantages[23] over discontinuous mode including better reproducibility and yields,[49,51–53] shorter development period and costs,[30] smaller equipment footprint[55] (up to 20% reduction in the CapEx)[23] and precise control of process parameters.[54] There are some challenges found in literature associated with the scale-up of continuous crystallization including fouling, clogging, and encrustation. Such events are predominantly caused by heterogeneous nucleation due to insufficient heat transfer or equipment material differences between scales.[50] A known example of a continuous crystallization plant in the industry is the Novartis-MIT Center of Continuous Manufacturing.[55,56] Rougeot *et al.*[15] described some examples where continuous preferential crystallization has been employed, emphasizing the advantages in process efficiency (**P6**).

Due to the complexity of crystallization, it is necessary the use of online analytical tools for real-time monitoring and control of the operation and to gather some data for a better process understanding. These tools are known as Process Analytical Technologies (PAT) and can be for example spectroscopy technologies as attenuated total reflectance (ATR) Fourier-transform infrared[57] or ATR-UV-Vis, NIR, Raman, or other techniques such as focused beam reflectance measurement[46,57–59] and particle vision and measurement.[57] In addition to the above widely used crystallization monitoring methods, conductivity, refractive index, turbidity measurements, are also available in PAT.[50] They are very important to monitor critical process parameters (CPPs) to control the critical quality attributes (CQAs).

In crystallization, PAT can be used to obtain *in situ* information about the solution and one important CPP is supersaturation because it can affect the nucleation, particle agglomeration, and crystal growth.[22,60] By using PAT, crystallization process development can be faster and reproducibility can be enhanced.[61,62] Continuous online monitoring was done

Open Access Article. Published on 20 May 2022. Downloaded on 14/09/2025 22:14:34.
This article is licensed under a Creative Commons Attribution-NonCommercial 3.0 Unported Licence.

for the resolution of (D/L)-threonine using an online polarimetric detector, a refractometer, and a density meter.[63,64]

Mixed-suspension mixed-product-removal (MSMPR) crystallizers. In the 1930s, mixed-suspension mixed-product-removal (MSMPR) crystallizers were developed.[50] They are a very common type of continuous crystallizers in industry and are frequently used for crystallization processes requiring long residence time. Mechanical stirring is usually applied to ensure uniform temperature and homogeneous mixing. Crystallization can be done in a single-stage or multiple stages. Single-stage MSMPR crystallizers are commonly used to study nucleation behavior or optimization of particle size distribution in continuous mode however, multiple-stage crystallizers connected through the liquid phase and operated under continuous exchange of crystal-free solution may significantly enhance yield, productivity, and product quality.[15,58,65]

The coupled preferential crystallizer (CPC) configuration is similar to coupled MSMPR except that there is no continuous feed and product removal.[66] The scale-up can be done by using pilot-scale stirred tanks and traditional equipment but some difficulties can be the lack of heat transfer in specific areas of the vessel and homogeneous mixing.[51] To improve yield, productivity, and quality, MSMPR crystallizers can be equipped with a recycle system[67] or they can be used in multiple stages where a cascade of several crystallizers are connected.[49]

Plug flow crystallizers. In the 1980s, plug flow crystallizers (PFCs) were developed. They are usually used for crystallization requiring shorter residence times and known to be very efficient in terms of heat and mass transfer and easier to scale up when compared to MSMPR or batch crystallizers.[50,62] PFCs also offer increased control compared with batch or MSMPR crystallizers in situations of very fast kinetics. The mixing rate is affected by the design of the crystallizer consisting of the piping components and format. Mixing elements such as Kenics type static mixers[59] can be included in the setup. There are different types of PFCs developed in the 1990s for example the continuous oscillatory baffled crystallizers that consist of a tubular crystallizer containing periodically spaced baffles with oscillatory motion on the net flow, increasing mass and heat transfer[68] and continuous segmented flow crystallizers where the solution inside the pipeline is divided by liquid "bubbles" in a continuous mode by an immiscible fluid producing crystals with precise particle size distribution and morphology.

Reviews comparing the differences between batch and continuous crystallizers and analysis of the advantages of each type have been reported.[22,50,62,69,70]

Fluidized bed crystallizers (FBC). In 1967 Midler *et al.*[71,72] described a robust continuous process for resolution of both enantiomers of (D/L)-*N*′-acetyl aminonitrile and (D/L)-acetamido-(*p*-hydroxyphenyl)-propionitrile, a precursor of the very known API α-methyl dopamine, with defined particle size distribution and purities higher than 97%. The authors employed two coupled conical-shaped fluidized bed crystallizers combined with continuous production of seed particles by using an ultrasonic probe to maintain the crystallization process in a steady state. Later, having in consideration Midler's process, the continuous resolution of 3-fluoroalanine-2-D benzenesulfonate salt was performed with 99.9% purity and 5.7 kg of the desired enantiomer was produced by Merck scientists.[73]

In a traditional procedure, a supersaturated solution is fed at the bottom of the crystallizer and this upward liquid flow agitates the crystals in the crystallizer to form a fluidized bed.[70] The flow exit at the top of the crystallizer. Seeds are generated by ultrasonication, at the bottom of the crystallizer. The conical shape of the crystallizer allows larger crystals to drop to the bottom, where they can be removed from the vessel. Moreover, since the fluidized bed crystallizer is conical at the lower part, the fluid flow velocity decreases with the increasing diameter which has a great impact on particle size.[74]

Operation setups. Studies on continuous preferential crystallization were mainly dedicated to introducing novel processing setups and operation modes, by using different kinds of reactors and by adding, for example, fine dissolution units or ultrasonic (Table 2). Additionally, evaluating the impact of process parameters (*e.g.*, continuous seeding and temperature cycling) to improve process stability by avoiding nucleation of the counter enantiomer and increase productivity and yields.[75]

Continuous preferential crystallization using a single crystallizer. Continuous preferential crystallization in one crystallizer is most like classical preferential crystallization.[15] In a single crystallizer, a racemic supersaturated solution is continuously fed and seeded with the pure desired enantiomer. The mother liquors are continuously removed to avoid the nucleation of the counter-enantiomer.

This method was first described in 1966 by Ito *et al.*[76] by using either a batch crystallizer or a fluidized bed crystallizer for the resolution of amino acids for example (D/L)-glutamic acid and (D/L)-threonine. Eicke *et al.*[77] showed the importance of fines dissolution on the delay of undesired nucleation of the counter-enantiomer and consequently increase the quality and purity of the desired enantiomer. This is accomplished through the use of mills or ultrasounds in the process.[16] In

Table 2 Inline methods to control nucleation and generating small crystals in continuous flow[70]

Inline methods	Purpose	Equipment	Crystallizer
Mixers	Mixing streams	Static mixers	PFC
Ultrasonication	Accelerate nucleation and crystal breakage	Sonicator	MSMPR, PFC; FBC
Milling	Crystal breakage	Rotor-stator mill	MSMPR
T cycling	Control undesired nucleation	Temperature control units	MSMPR, PFC; FBC
Recycling	Increase yield	Filters, columns, membranes	MSMPR, FBC

 This journal is © The Royal Society of Chemistry 2022

Open Access Article. Published on 20 May 2022. Downloaded on 14/09/2025 22:14:34.
This article is licensed under a Creative Commons Attribution-NonCommercial 3.0 Unported Licence.

2012, Qamar *et al.*[78] mathematically described for the first time continuous preferential enantioselective crystallization using a single crystallizer equipped with a fines dissolution unit (Fig. 2 and Table 3).

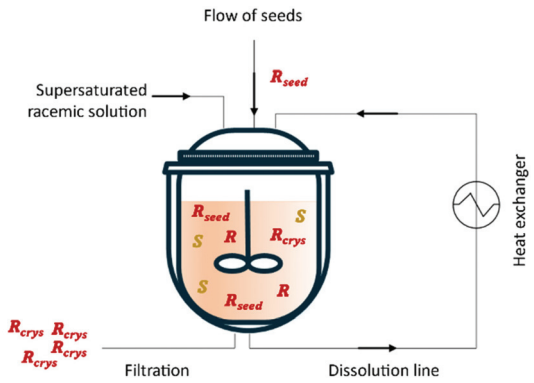

Fig. 2 Illustration of a simple continuous procedure for an enantiomeric resolution using a single crystallizer. Adapted from ref. 78.

Kollges *et al.*[75] designed a crystallizer unit that is continuously fed with a supersaturated solution of racemic composition. Provision of seed crystals with an enriched composition during the startup phase and by selecting appropriate feed concentration and residence time, a steady state with pure solid phase composition can be obtained from the MSMPR crystallizer. The suspension is continuously transferred into the filtration unit where the solids are separated from the solution. The mother liquor resulting from the filtration is recycled back. The system operates with a distillation system to remove a determined amount of the solvent and maintain the level of the reactor (Fig. 3 and Table 3).

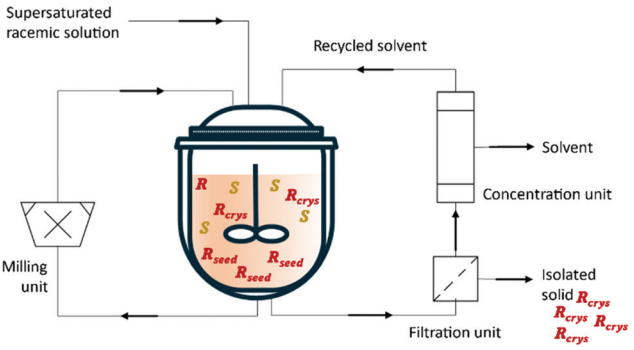

Fig. 3 Illustration of a continuous preferential crystallization with mother liquor recycling and a milling unit for large crystals breakage and fines dissolution. Adapted from ref. 75.

To prevent waste (**P1**), the distilled solvent might be used for future trials. Moreover, the distillation system could be substituted by a nanofiltration membranes system (**P6**) where the retentate would be fed back into the crystallizer and the permeate could be recycled for future trials.

Continuous preferential crystallization using two-coupled crystallizers. To enhance the productivity of the preferential crystallization, in 2007 Elsner *et al.*[83] proposed the simultaneous crystallization of both enantiomers in two separated vessels with an exchange of crystal-free mother liquor. Both vessels are continuously fed with a racemic supersaturated solution and seeded separately with one of the two enantiomers. To minimize the probability of primary nucleation of the counter-enantiomer, while the preferential crystallization occurs, the mother liquors must be continuously exchanged between crystallizers. Therefore, the enantiomeric excess of one enantiomer in the mother liquors created by the preferential crystallization of the counter-enantiomer is instantly eliminated by exchanging the mother liquor to the opposite crystallizer. Because of this swap, the liquid phase shows a higher overall concentration of the preferred enantiomer in that vessel in which the preferred enantiomer was seeded and the concentration of the counter enantiomer in the mother liquors of each vessel decreases.[84,85] Theoretical study of the preferential crystallization in two-coupled MSMPR crystallizers was reported by Elsner *et al.*[83] and Qamar *et al.*[86,86] (Fig. 4). In 2012, Levilain, Eicke *et al.*[87,88] proposed a variant approach named *Coupling Preferential Crystallization and Dissolution* based on the exchange of liquid phases between two tanks that are operated at two different temperatures and requiring seeds of only one enantiomer, which keeps the investment at a lower level. Temmel *et al.*[89] described the process development of Racemic Guaifenesin using this approach in batch mode.

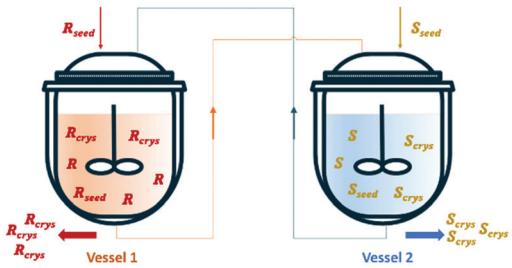

Fig. 4 Illustration of a simultaneous preferential crystallization with two vessels coupled *via* mother liquors exchange. Adapted from ref. 83.

Vetter *et al.*[16] coupled two continuous crystallizers by exchanging their clear liquid phases. Each crystallizer was connected to a grinder responsible for *in situ* seed generation through large crystals breakage. The authors concluded that, by using this setup, it is possible to continuously obtain the desired enantiomer in one crystallizer and the counter-enantiomer in the other. They determined that an enantiomerically pure steady state can be obtained. Moreover, the process also recovers from the sudden appearance of undesired crystals of the counter-enantiomer, which is a phenomenon encountered from time to time in industrial crystallizers due to scale formation at the crystallizer walls.

Qamar *et al.*[65,78] developed mathematical models exploiting the dynamics of continuously operated single and two-coupled

Open Access Article. Published on 20 May 2022. Downloaded on 14/09/2025 22:14:34.
This article is licensed under a Creative Commons Attribution-NonCommercial 3.0 Unported Licence.

Table 3 Overview of reported model-based continuous preferential crystallization

Authors	Type of crystallizer	Substance	Studied parameters	Findings	Year	Ref.
Qamar *et al.*	Single-MSMPR with fines dissolution	D/L-Thr	Continuous seeding without fines dissolution; continuous seeding with fines dissolution; effect of the ratio between solid and liquid phases	This model can be used to find the optimum operating conditions for improving the product quality and for reducing the operational cost of continuous preferential crystallization	2012	78
Qamar *et al.*	Two-coupled MSMPR with fines dissolution	D/L-Thr	Continuous seeding without fines dissolution; continuous seeding with fines dissolution; periodic seeding without fines dissolution	Significant improvements were achieved by using two coupled MSMPR when compared to a single-MSMPR. This model can be used to find the optimum operating conditions for improving the product quality and for reducing the operational cost of continuous preferential crystallization	2013	65
Chaaban *et al.*	Two-coupled MSMPR with a feed tank	D/L-Asn	Mean residence time of the liquid phase; fraction of the feed solution inlet; amount, average particle size, and morphological effects of seeds	A mathematical model describing the resolution of (D/L)-asparagine in two-coupled MSMPR and a feed tank under isothermal conditions was developed. It was shown that the increase in the mean residence time of the liquid phase, the increase in the mass of seeds, and the reduction of the size of the seed crystals all contribute positively to the overall process performance	2014	79
Köllges *et al.*	MSMPRC *via* Viedma Ripening with mill unit	Generic	Process configuration using different crystallization techniques: (1) resolution *via* preferential crystallization and (2) deracemization *via* Viedma Ripening	The configuration (1) achieves the complete separation of enantiomers of a conglomerate forming system using a single-MSMPR. Configuration (2) obtained an enrichment of roughly 90% ee but requires excessively long residence times with correspondingly low productivities to achieve this	2017	80
Mangold M. *et al.*	FB with a mill unit	Generic	Influence of the fluid and product flow rate; influence of the flow rate to the mill and its properties; influence of the crystallizer geometry; influence of the crystal growth rate	It is found that the inlet flow rate has a strong influence on productivity; the product flow rate hardly influences the productivity; more effective means to change the product size distribution are modifications of the crystallizer geometry; and modifications of the mill affecting the size distribution of the seeds	2017	81
Kollges *et al.*	MSMPRC with recycling and solvent removal; MSMPRC *via* Viedma Ripening with a pre-crystallizer	Generic	Process configuration using different crystallization techniques: (1) resolution *via* preferential crystallization and (2) deracemization *via* Viedma Ripening	two MSMPRC cascades with equal residence times perform worse than the two MSMPRC cascade with variable residence times unless a very high enantiomeric purity is demanded; adding further crystallizers does not boost the productivity substantially for the variable residence time case; in the case of equal-sized MSMPRCs, the PC process outperforms the processes that rely on ripening stages in terms of productivity	2018	75
Mangold M. *et al.*	FB with a mill unit	Generic	Particle velocity profiles at different positions in the crystallizer for a constant liquid flow rate crystal phase purity; minimum operation flow rate	The linear model studied can be useful for process optimization or control purposes	2020	82

MSMPR crystallizers equipped with a fines dissolution system. The authors used available solubility and kinetic data of (D/L)-threonine in water systems and carried out simulation studies. The impact of different seeding strategies and residence time distributions on the yield, purity, productivity, and crystal size was investigated (Table 3 and Fig. 5).

 This journal is © The Royal Society of Chemistry 2022

Open Access Article. Published on 20 May 2022. Downloaded on 14/09/2025 22:14:34.
This article is licensed under a Creative Commons Attribution-NonCommercial 3.0 Unported Licence.

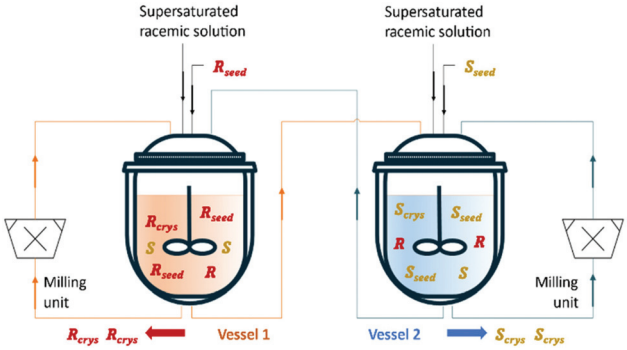

Fig. 5 Illustration of a simultaneous preferential crystallization with two vessels coupled *via* mother liquors exchange and milling units for large crystals breakage and fines dissolution. Adapted from ref. 65.

Later, Galan *et al.*[51] investigated experimentally and compared the separation of (D/L)-threonine using continuous operated single MSMPR crystallizer and two-coupled MSMPR with continuous exchange of mother liquors. The co-workers used Qamar process models to identify suitable operating conditions. Although it was possible to perform continuous preferential crystallization using a single MSMPR crystallizer, under identical conditions almost the double of productivity was achieved by using two-coupled MSMPR vessels, at the same high level for both configurations. Furthermore, the two-coupled MSMPR allowed harvesting both enantiomers simultaneously. Majumder *et al.*[66] also studied the resolution of (D/L)-threonine in the water system. A detailed study on the effect of process parameters (*e.g.*, feed flow rate, seed mass, and liquid phase exchange) on productivity and yield was presented. Both works have achieved enantiomeric excess >99% for the L-enantiomer.

Chaaban *et al.*[53,79] achieved a continuous preferential crystallization of (D/L)-asparagine monohydrate in water using a two-stage MSMPR crystallizer coupled *via* mother liquors exchange. They showed, by mathematical modeling and validation, how productivities, yields, and purities of solid products were influenced by the morphological differences in the seed crystals. Final purities of 100% and productivity of 0.94 g L^{-1} h^{-1} were obtained for each enantiomer (Table 3).

In the described processes, the maximum isolated yield obtained is 50% for the desired enantiomer, leading to a poor atom economy (**P2**) and the generation of a high amount of waste (**P1**). A great option would be the racemization of the undesired enantiomer and future preferential crystallization of the obtained racemic mixture to increase the yield and atom economy. Moreover, the Viedma Ripening procedure could be used for the achievement of 100% theoretical yield.

Hein *et al.*[93] proposed a method based on the attrition-enhanced deracemization (Viedma Ripening) approach where preferential crystallization occurs in one vessel and selective dissolution of the counter-enantiomer in the second vessel. The authors successfully obtained *S*-omeprazole with a productivity of 0.84 g L^{-1} h^{-1} and 98% purity.

Additionally, the authors showed how this procedure can be applied for continuous resolution of the (D/L)-threonine system. Obtaining enantiopure L and D enantiomers separately with 76% and 79% yields, respectively (Fig. 6).

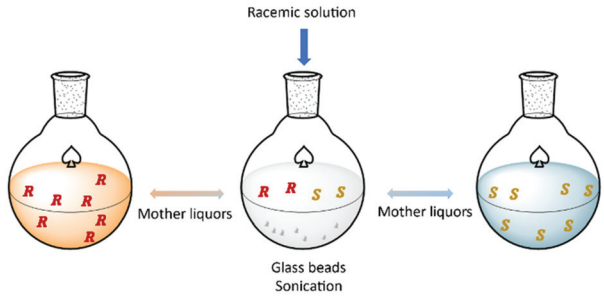

Fig. 6 Schematic illustration of coupled preferential crystallization using attrition. Adapted from ref. 93.

Kollges *et al.*[75] designed a continuous Viedma Ripening process where a pre-crystallization step (it generates a racemic mixture of crystals) is followed by one or more ripening stages that successively increase the enantiomeric excess. In the pre-crystallization unit, the mother liquors are filtered, concentrated, and recycled into the vessel. It also has a milling unit to provide attrition. Following the ripening stage, the final solid containing high enantiomeric excess is filtered in a second filtration unit and the mother liquors are recycled back to the first ripening stage (Table 3).

In 2018, Majumder proposed a novel PFC configuration involving two coupled PFCs with liquid phase exchange. Simulation studies were carried out using (D/L)-threonine in a water system as a model. The author used a set of coupled population balance equations to describe the evolution of the crystal phase of both enantiomers in each crystallizer. The results predict that the proposed configuration has higher productivity compared to the currently used continuous crystallization configurations (MSMPR and single-PFC) while maintaining the same level of purity (Table 4 and Fig. 7).[91]

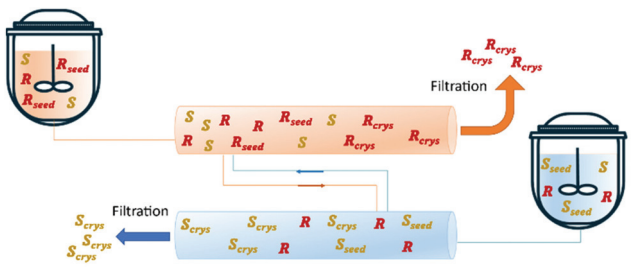

Fig. 7 Illustration of coupled plug flow crystallizer *via* mother liquor exchange. Adapted from ref. 91.

Recently, Cameli *et al.*[54] reported the continuous preferential crystallization of isoindoline-1-ones derivatives using a plug flow crystallizer immersed in two thermostatic baths set at different temperatures. This configuration allowed them to obtain productivities of 20 g L^{-1} h^{-1} due to the excellent heat transfer and low residence periods (Table 4 and Fig. 8).

Open Access Article. Published on 20 May 2022. Downloaded on 14/09/2025 22:14:34.
This article is licensed under a Creative Commons Attribution-NonCommercial 3.0 Unported Licence.

Table 4 Reported purity and productivity of continuous preferential crystallization of enantiomers[a]

Product	Type of crystallizer	Technique	Purity (%)	Productivity (g L^{-1} h^{-1})	Ref.
(D/L)-Asparagine monohydrate	Fluidized bed crystallizers	Two-coupled FBC	97.0	14	90
			97.0	40	52
	MSMPR	Two-coupled MSMPR	100	0.94	53
			100	0.38	30
(D/L)-Threonine	MSMPR	Single MSMPR	98.8	3.2	51
		Two-coupled MSMPR	99.3	6.3	
		Two-coupled MSMPR	99.0	7.7[b]	66
	Plug flow crystallizer (PFC)	Single PFC	99.0	9.3[b]	91
		Two-coupled PFC	99.0	13.3[b]	
Omeprazole	MSMPR	Two-coupled MSMPR	98.0	0.84	92
Indoline derivatives	Plug flow crystallizer	Two-coupled PFC	98.0	20	54

[a] We always picked the best-case scenario reported in each article. [b] Calculated by having into consideration the feed flow rate.

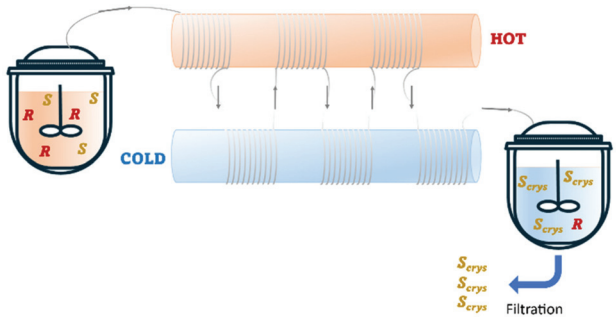

Fig. 8 Illustration of a plug flow crystallizer with hot and cold zones for dissolution and re-crystallization, respectively. Adapted from ref. 54.

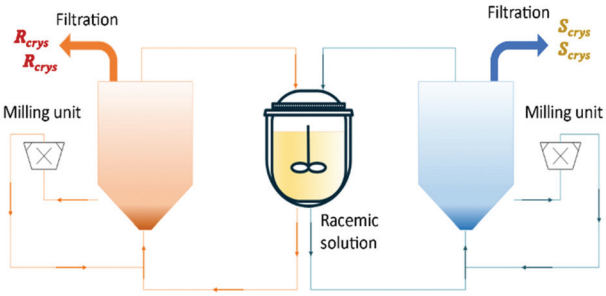

Fig. 9 Illustration of coupled tubular fluidized bed crystallizers with a conical lower section and milling units for crystal breakage and fines dissolution. Adapted from ref. 90.

Binev *et al.*[90] and Temmel *et al.*[52] studied the feasibility of a fluidized bed process with two coupled crystallizers for continuous preferential crystallization of a racemic mixture of (D/L)-asparagine monohydrate (L-asn·H_2O) in water. The first authors obtained final purities up to 97% and productivities up to 14 g L^{-1} h^{-1} for each enantiomer (Table 4). The second authors also obtained final purities up to 97% but productivities up to 40 g L^{-1} h^{-1} for each enantiomer.

In this process, the seed crystals move continuously through the fluidized crystal bed until they are grown to a size at which they settle at the bottom of the fluidized bed. Then, they are removed *via* peristaltic pumps into a bypass and flow through high-speed dispersers, which were utilized as mills. After that, the milled crystals are feedback as seed material to the process. The authors showed how important it is the effect of the conically shaped tubular crystallizers in the crystal size distribution, low fine contents, high purities, and robust production (Fig. 9).

Mangold *et al.*[81] presented a mathematical process model based on population balance equations for a continuous fluidized bed crystallizer, they identified the key operation and design parameters for maximizing the productivity and better control of crystal size distribution (Table 3).

Other approaches are described for example for the resolution of a racemic mixture of menthyl benzoate on a scale of 300 kg h^{-1} where a new type of crystallization apparatus is described.[94] A further variation involves a three-container system of two coupled crystallizers and a feed tank. This setup relies on simultaneous preferential crystallization of both enantiomers in parallel into the two crystallizers, while the racemic mixture is progressively dissolved from the dissolver tank.

Sustainability considerations. Preferential Crystallization is a cost-effective method to obtain crystals of a single enantiomer from a racemic solution but is limited to chiral systems that occur as a conglomerate.

Continuous preferential crystallization has gained interest due to its many advantages over discontinuous mode including better reproducibility, yields, and precise control of process parameters. Moreover, it can offer reduced capital expenditure (CapEx) and operational expenditure (OpEx) along with the more efficient use of energy and materials (**P1** and **P6**).[20]

When comparing both procedures of preferential crystallization and Pasteurian resolution, there is no doubt that the first method is greener. It does not involve additional chemical steps by firstly forming diastereomers salts for the crystallization procedure and secondly, forming the desired enantiomer at the end of the process. When preferential crystallization is used, the atom economy (**P2**) is higher, and the energy/material efficiency is increased.

A possibility to make the resolution greener and increase the inherently maximum 50% yield would be to racemize the isolated undesired enantiomer after preferential crystallization. Consequently, obtaining a racemic solution that would be fed into the crystallizer.

Open Access Article. Published on 20 May 2022. Downloaded on 14/09/2025 22:14:34.
This article is licensed under a Creative Commons Attribution-NonCommercial 3.0 Unported Licence.

3. Membrane-based chiral separation

Membrane-based chiral separation is a promising low-cost technique for efficient separation of enantiomers due to its intrinsic advantages such as being operated in continuous mode, low energy consumption (**P6**), high efficiency of the resolution, and ease of scale-up.[95,96] Moreover, it should offer a good transport rate with high selectivity, to be stable in a high range of pH and compatible with different types of solvents.[97] The membrane act as a barrier and may selectively transport one enantiomer due to specific interactions (hydrogen bonding, coulombic or van der Waals) between the enantiomer molecule and a chiral recognition site of the membrane, thus producing a permeate solution enriched with this specific enantiomer. Within the last decades, a large variety of synthetic membranes were developed for specific process optimization. They can be classified according to their backbone material, their morphology, preparation method, and shape.[98]

An efficient separation can be achieved by using an enantioselective liquid or solid membrane that contains a chiral recognition site that may be a chiral side chain, a chiral backbone, or an immobilized chiral selector. Also, a non-enantioselective solid membrane with a specific molecular weight cut-off (MWCO) can be used for nano or ultrafiltration procedures where the preferred enantiomer may complex with a specific chiral selector before filtration. Therefore, the resolution method for non-enantioselective membranes is different from enantioselective membranes.[95,99]

The membrane properties that determine the feasibility and characteristics of the processes are permeability and selectivity. The permeability of a membrane is defined as the normalized flux regarding the concentration change and the thickness of the membrane. The selectivity of a membrane is defined as the permeability ratio of the compounds of interest, in this case, the two enantiomers.[98]

The selectivity of the process can be calculated in terms of enantiomeric excess (ee) and separation factor (α).

$$\mathrm{ee}\% = \frac{C_R - C_S}{C_R + C_S} \times 100$$

where C_R and C_S refer to the concentration of the *R* and *S* enantiomers, respectively. And

$$\alpha = \frac{J_R}{J_S}$$

where J_R and J_S are the normalized flux of the *R* and *S* enantiomers, respectively that can be calculated following the formula below.

$$J = \frac{\Delta CV}{\Delta tA}$$

where ΔC is the concentration difference of each enantiomer, Δt is the permeation time, V is the downstream volume, and A is the effective membrane area.

The transport process through the membranes can be categorized as filtration, dialysis, electrodialysis, and pervaporation. Several factors can influence the transport mechanism, it depends on the main driving force of the permeation of compounds through the membranes such as binding affinity forces, pressure gradient, solutions concentration, and electric field or vapor difference.[100]

The two transport mechanisms can be categorized as facilitated (diffusion-selective membranes) or retarded (sorption-selective membranes). An enantioselective membrane preferentially allows a specific enantiomer to adsorb or to diffuse into the membrane. In diffusion selective membranes, one enantiomer is preferentially adsorbed into the chiral recognition sites, and it is continuously adsorbed and de-adsorbed from one site to the next, and finally it reaches the stripping phase by increasing driving forces such as pressure or pH. The other enantiomer, which has no affinity to the chiral sites, passes through the membrane by diffusion.[98] Mostly chiral liquid and solid membranes built from a chiral polymer or coated with an enantioselective polymeric thin-layer employ facilitated transport.[99] Sorption selective membranes, which selectively absorb and immobilize one of the enantiomers through incorporated chiral selectors while permitting the other to flow due to lower affinity to the carrier, normally are built from porous membrane material.[101] Since the bound with the enantiomer is stronger and the selectivity can be maintained with the convective flow, these types of membranes are more attractive commercially.[102]

In 1980, the first example of enantiomers separation by host–guest complexation was described by Cram *et al.*[103–105] The authors developed an enantioselective extraction procedure using crown ethers as chiral selectors in chloroform. Examples of chiral selectors can be found in the literature namely different types of cyclodextrins, albumin or other proteins, chiral polysaccharide chains like chitosan or sodium alginate, DNA, crown ether derivatives, and oligopeptides.[100,106] In 1990, Pirkle *et al.*[107] patented an invention related to a continuous process to separate enantiomers by using a supported liquid membrane and a chiral carrier that selectively complexes with one of the two enantiomers.

3.1. Liquid membranes for chiral resolution

Liquid membranes consist of a liquid phase that acts as a membrane between two fluid phases.[108] Chiral liquid membrane technology has been extensively investigated for the separation of enantiomers due to its high separation factor and increased mass transfer as a result of the higher solubility and diffusivity coefficients of compounds in a liquid medium than in a solid membrane.[97] The three basic types of liquid membranes are supported liquid membrane (SLM), emulsion liquid membrane (ELM), and bulk liquid membrane (BLM) – Fig. 10.

Bulk liquid membrane. Bulk Liquid Membranes (BLM) consists of an immiscible liquid phase that acts as a membrane between the feed and receiving phases and it is where the chiral selector must be dissolved. One enantiomer of the pair

Open Access Article. Published on 20 May 2022. Downloaded on 14/09/2025 22:14:34.
This article is licensed under a Creative Commons Attribution-NonCommercial 3.0 Unported Licence.

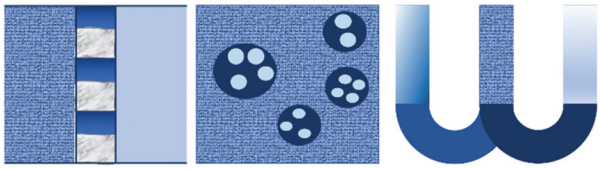

Fig. 10 Illustration of different types of liquid membranes. Adapted from ref. 97.

is preferentially transported by the chiral selectors in the liquid membrane to the receiving phase usually in the presence of a pH or concentration gradient.[95,109] A careful selection of the chiral carrier must be done because it has to preferentially bind one of the two enantiomers. Also, the solubility of the carrier (and consequently the formed complex) in the feed, membrane phase, and receiving phase must be determined. The carrier and formed complex must only be soluble in the membrane phase and the enantiomers must be soluble only in the feed and receiving phase.[97] The low specific interface area of the BLM leads to low mass transfer rates limiting the application of this technology at an industrial scale. Nevertheless, BLMs can still be used on a laboratory scale and to screen different chiral selectors.[108]

The set-up is known as the "resolving machine" developed by Cram *et al.*[105] consists of two U-tube containing different selectors for each enantiomer in chlorinated solvents (Fig. 11). The outcome is that the (*R*)-enantiomer will be in a receiving phase different than the (*S*)-enantiomer.

Feringa *et al.*[110] worked on the separation of amino acid enantiomers using Palladium (*S*)-BINAP complexes as chiral carriers using the "resolving machine". One advantage of this process is that the host can be prepared *in situ* from commercially available compounds. The system also showed a great selectivity for Tryptophan.

Krieg *et al.*[111] described the resolution of racemic chlorthalidone using a U-tube multiple membrane cell consisting of three membrane phases and three stripping phases with β-cyclodextrin as chiral selector.

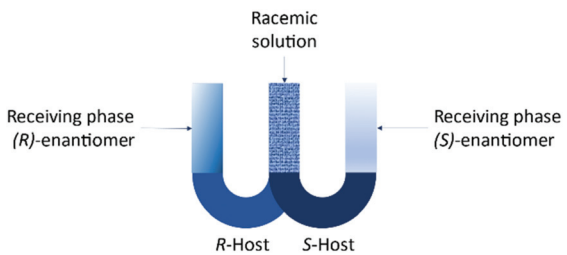

Fig. 11 Resolving machine developed by Cram *et al.*[105]

Emulsion liquid membrane. Emulsion liquid membranes (ELMs) or liquid surfactant membranes provide the highest mass transfer rates among the other types of liquid membranes, due to their high surface area to volume ratios.[108] ELMs can be operated continuously, and are scalable. Nevertheless, could be possible to occur emulsion swelling and leakage, which may decrease the efficiency and selectivity.[95,112,113] In ELM systems, the aqueous feed phase is typically dispersed in an organic membrane phase (spherical membrane globules), which is dispersed into an aqueous receiving phase (a double emulsion).[114] Recovery of the extracted compounds from the receiving phase is caused by applying a pH, concentration, or temperature gradient.

To obtain (D)-phenylalanine from a racemic mixture, Pickering *et al.*[112,115] developed a chiral ELM using copper(II) *N*′-decyl-(L)-hydroxyproline as chiral selector in a mixture of decane/hexanol. An enantiomeric excess of 40% was obtained. Huang *et al.*[116] reported the resolution of racemic α-cyclohexyl mandelic acid across microemulsion liquid membranes system using tartaric acid benzyl ester as chiral selector, sodium dodecyl sulfate as the surfactant, and mixture *n*-butyl alcohol and *n*-heptane as the organic solvents. The effect of several variables such as chiral selector concentration, pH value in the external aqueous phase, and volume ratio of the external aqueous phase to membrane phase was studied. The maximum separation factor obtained was up to 2.0.

In the referred cases, some use metallic chiral selectors. For toxicological, environmental, and economic reasons, it should be avoided and substituted for environmentally friendly hosts (**P3**).

Supported liquid membranes. SLM has attracted much attention in recent years due to its advantages of high selectivity and high throughput. Compared with bulk liquid membrane and emulsion liquid membrane, SLM presents easier scaling-up and low operating costs.[117] They are the most used liquid membranes for the separation of chiral compounds. The membrane consists of a porous inert backbone immersed in a water-immiscible solvent in which a chiral selector is dissolved. Generally, hydrophobic materials such as polyethylene, polypropylene, or polytetrafluoroethylene are used.[118] The membrane liquid should be permeable to the enantiomers to be separated, but not for the chiral selector. To avoid the transport of chiral selector molecules over the racemic solution, the selector must be highly lipophilic. It was described several case studies on the separation of aminoacids[119–121] and drugs[122–124] enantiomers using SLMs. Hollow-fiber membranes are a type of SLMs with high surface area per volume, thus resulting in a relatively compact system.[96] A common approach when using a hollow fiber module is to feed a solution of the chiral selector in a water-immiscible solvent through the interior of the fibers (lumen/shell side), while the aqueous-feed stream that contains the racemic substrate circulates in the stripping side of the hollow-fiber module.[125]

Hollow fiber membranes. Enantioselective membranes can resolve optical isomers due to chiral properties such as chiral recognition sites (*e.g.*, chiral side chains, chiral backbones, or chiral selectors). Although, it is possible to use membranes that are not enantioselective but has specific properties that allow an efficient separation such as hollow-fiber membranes.[118] In one of the most common approaches, a solution of the chiral selector (*e.g.*, cyclodextrins, polysaccharides, *etc.*)

Open Access Article. Published on 20 May 2022. Downloaded on 14/09/2025 22:14:34.
This article is licensed under a Creative Commons Attribution-NonCommercial 3.0 Unported Licence.

in a water-immiscible solvent is fed through the interior of the fibers of the membrane while the aqueous feed containing the racemic compound circulates in the shell side of the hollow-fiber module in countercurrent flow (Fig. 12).[125] When the two phases flow in counter current, any desired degree of separation can be achieved.[96]

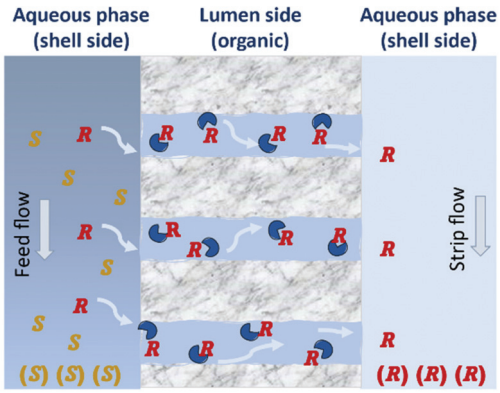

Fig. 12 Principle of enantiomeric separation by hollow-fiber membranes. The (*R*)-enantiomers are being transported through the membrane by diffusion. Adapted from ref. 125.

The use of hollow fiber membranes usually results in a relatively compact system because of a high membrane surface area per volume.[96] Several case studies are found in the literature demonstrating how the solute exchange between two crystallizers separated by a hollow-fiber membrane module results in both high purity and high yield.[126,127] Moreover, a series of membranes can be used for a better efficient mass transfer.[128] In 1992, Cussler *et al.*[129] described the separation of Leucine enantiomers with an enantiomeric excess of 99% by fractional extraction across microporous hollow fibers (Fig. 13). The authors considered the two-phase system for enantioselective separation developed by Takeuchi *et al.*[130]

Firstly, the water-immiscible solution (*N*′-decyl-(L)-hydroxyproline in octanol) is fed into the column on the shell side. Then, the aqueous phase is fed into the lumen side in counter current. When a stationary state is reached in both the lumen and shell side, the feed flow consisting of a racemic solution of leucine is feed. The enantiomers are collected in opposite leaving streams of the column and quantified by chromatography.

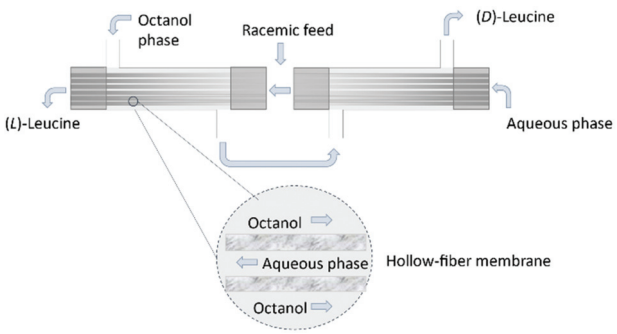

Fig. 13 Separation of leucine enantiomers in a hollow fiber module. Shell side: octanol, lumen side: aqueous solution. Leucine enantiomers are collected in the exit streams of the module. Adapted from ref. 129.

Four years later, Keurentjes *et al.*[96] determined the enantioselectivity for Ibuprofen, Salbutamol, Propanolol, Norephedrine, Ephedrine, Mirtazapine, Phenylglycine and Terbutaline testing different chiral selectors solutions, namely (*R*,*R*)/(*S*,*S*)-di-hexyltartrate and dibenzoyl tartaric acid in heptane or chloroform, and different lipophilic anions to form complexes with the racemates to increase drug solubility. The modules were built with regenerated cellulose hollow-fiber membranes. Norephedrine was obtained with an enantiomeric excess of 99% (Table 5).

Hadik *et al.*[131,132] reported the resolution of (D/L)-lactic acid and (D/L)-alanine by using *N*′-3,5-dinitrobenzoy-(L)-alanine-octylester as the chiral selector. The authors compared the enantiomeric resolution capability of a hollow fiber-supported liquid membrane and a chiral solid membrane. On one hand, the maximum enantiomeric excess obtained was 33.5% for (D)-lactic acid and 27.2% for (D)-alanine when SLM was used. On the other hand, when using a chiral solid membrane, the maximum enantiomeric excess obtained was 100% for (D)-lactic acid but no separation of Alanine enantiomers was achieved.

Supported hollow fiber membranes can be used in series for a better process efficiency and productivity. In 2006, Maximini *et al.*[128] developed a continuous SLM system (two in series) to separate enantiomers of racemic *N*′-protected amino acid derivatives using carbamylated quinine and quinidine derivatives as chiral selectors. Wang *et al.*[133] developed a process to separate ketoconazole enantiomers using a hydrophobic chiral selector – isopentyl tartrate which will recognize (2*R*,4*S*)-ketoconazole – in the organic phase (shell side) and a hydrophilic chiral selector – sulfobutylether-β-cyclodextrin in the aqueous phase (lumen side) which will recognize (2*S*,4*R*)-ketoconazole. The optical purity for the enantiomers is up to 90% when used two modules in series.

Prapasawat *et al.*[134] modeled and validated the resolution of racemic phenylalanine using *O*,*O*-dibenzoy-(L)-(2*S*,3*S*)-tartaric acid (DBTA) as chiral selector. Several parameters were investigated, such as concentration of DBTA and feed solution, initial pH, and equal flow rates of feed and stripping solutions. 55% of enantiomeric excess was obtained for (L)-phenylalanine at pH 5.

Svang-Ariyaskul *et al.*[126,135,136] reported the resolution of (D/L)-glutamic acid using a hybrid system where two streams are recirculated in two crystallization vessels and feed in countercurrent in a hollow-fiber membrane module, which allowed solute interchange between the vessels but a limited transfer of crystals. Each crystallizer contained a racemic solution of glutamic acid. Seed crystals of a specific enantiomer were fed to one of the crystallizers when the solution was at or near saturation conditions, while seed crystals of the opposite enantiomer were added to the other crystallizer. The feasibility of the process was demonstrated, and key operating variables were

Open Access Article. Published on 20 May 2022. Downloaded on 14/09/2025 22:14:34.
This article is licensed under a Creative Commons Attribution-NonCommercial 3.0 Unported Licence.

Table 5 Overview of published case studies that use hollow-fiber modules for enantiomeric resolution

Hollow fiber material	Membrane solution phase	Compound	Enantiomeric excess (ee) and/or separation factor (α)	Ref.
Polypropylene cross-linked with polyvinyl alcohol gel	Dodecyl-hydroxyproline and octanol	Leucine	99%	129
Regenerated cellulose (RC)	10 wt% di-hexyl tartrate (DHT) in heptane	Norephedrine	>99%	96
Polyacrylonitrile enzyme activated membrane	Toluene	Diltiazem intermediate	85%	137
Polypropylene	*N*-3,5-Dinitrobenzoyl-alanine-octyl ester in toluene	Lactic acid Alanine	33.50% (α: 2.00) 27.17% (α: 1.75)	131
Polypropylene	*N*-3,5-Dinitrobenzoyl-alanine-octylester in toluene	Lactic acid	34.60%	132
Polysulfone	Adamantyl-carbamoyl-11-octadecylthio ether-quinine in 1-decanole/pentadecane	*N*-Protected amino acid derivatives (DNB-(D/L)-leucine)	98%	128
Polyvinylidene fluoride	Isopentyl tartrate, sulfobutylether-cyclodextrin	Ketoconazole	90%	133
Polypropylene	DBTA in octanol	Phenylalanine	55%	134
Polysulfone	Exchanging mother-liquors	Glutamic acid	99%	126, 135 and 136
Polypropylene	DBTA in 1-decanol	Amlodipine	40.4%	139
Polypropylene	DBTA in 1-decanol	Cetirizine	75%	140
Polypropylene (asymmetric synthesis)	Undecane	1-Methyl-3-phenylpropyl-amine	98%	138
Polyvinylidene fluoride coated with molecularly imprinted polymer	MAA + EGDMA + *S*-ADB	Amlodipine besylate	90% (α: 1.98)	141
Polyvinylidene fluoride	(D)-Tartaric acid and a commercial extractant in heptane	Amlodipine	90.7%	127

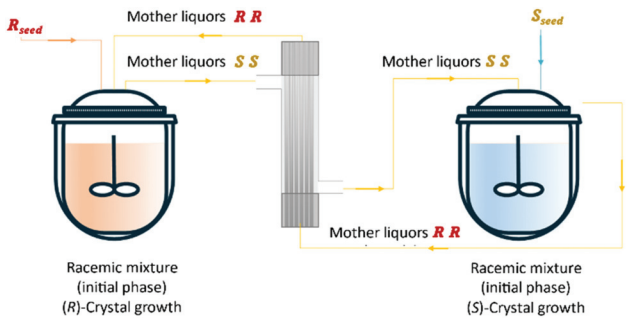

Fig. 14 Schematic representation of the hybrid crystallization/filtration process. By seeding the vessels, it will promote the preferential crystallization of a specific enantiomer. The counter enantiomer rich mother liquors will flow through the membrane only transporting the dissolved compounds.

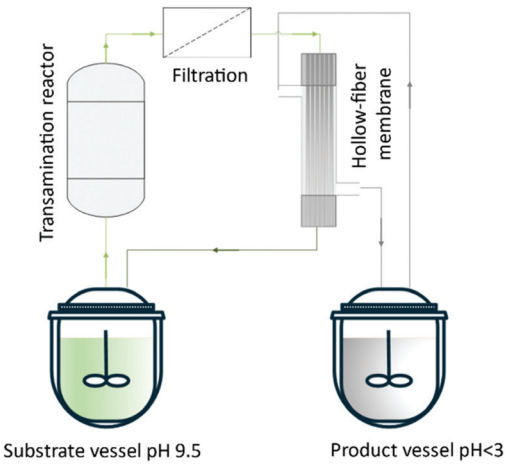

Fig. 15 System to produce 1-methyl-3-propylamine (MPPA) from (L)-alanine and benzylacetone. The system consists of a transamination reactor containing an immobilized enzyme, an in-line filter and a hollow-fiber module that separates the product from a co-product by a pH differential of lumen/shell sides.

identified. The enantiomeric excess of 99% of both enantiomers was obtained (Fig. 14).

Lopez *et al.*[137] described a hollow-fiber membrane reactor to an enzyme-mediated resolution of a racemic mixture of a Diltiazem intermediate. The authors developed the process from bench-scale to pilot plant. They built a reactor containing hydrophilic enzyme-activated porous located at the interface between organic and aqueous streams. Thus, the hollow fibers were used to 'immobilize' the biocatalyst and allow the enzyme phase to be in contact with the substrate organic phase. Börner *et al.*[138] reported the amine transaminase-catalyzed synthesis of chiral amines. The authors investigated the feasibility of using alanine as an amine donor for the reductive amination of a poorly water-soluble ketone in combination with the SLM strategy for *in situ* product removal. The amine product (1-methyl-3-phenylpropylamine) was obtained with enantiomeric excess above 98% without any additional purification (Fig. 15).

Sunsandee *et al.*[139,140] studied the enantioselective separation of (*S*)-amlodipine and (*S*)-cetirizine *via* a hollow fiber-supported liquid membrane. In both cases, DBTA was used as a chiral selector in 1-decanol. The maximum enantiomeric excess

Open Access Article. Published on 20 May 2022. Downloaded on 14/09/2025 22:14:34.
This article is licensed under a Creative Commons Attribution-NonCommercial 3.0 Unported Licence.

obtained for (*S*)-amlodipine was 40.5% and for (*S*)-cetirizine was 75%.

To promote the selectivity of hollow fiber, molecularly imprinted hollow-fiber membranes can be prepared by immobilizing the molecularly imprinted layer on the cavities of the hollow-fiber *via* an interfacial polymerization technique. Lai *et al.*[141] prepared molecularly imprinted hollow fiber membranes with methacrylic acid (MAA) as the functional monomer, ethylene glycol dimethacrylate (EGDMA) as the cross-linker, and (*S*)-amlodipine as an imprinted template. As a result, (*S*)-amlodipine was obtained with 90% enantiomeric excess and a separation factor of 1.98.

Recently, Zeng *et al.*[127] developed a novel method for the enantioseparation of Amlodipine using a hollow fiber module as an extraction and crystallization system. For the extraction operation, the authors used a commercial extractant P507 (2-ethylhexyl phosphonic acid mono-2-ethylhexyl ester and heptane and for the crystallization operation, (D)-tartaric acid as the chiral selector and DMSO as antisolvent. The obtained enantiomeric excess was 90.7% and a global yield of 48.8% for the isolated product, (*S*)-amlodipine (Fig. 16).

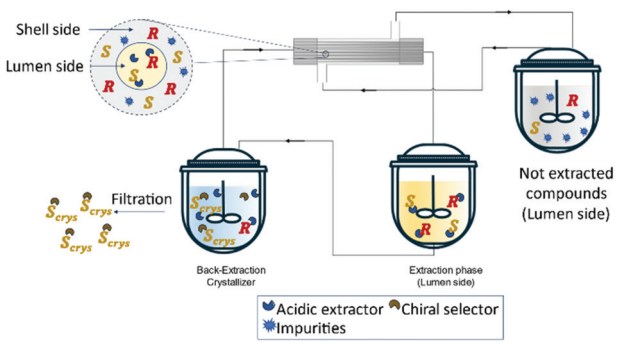

Fig. 16 Schematic representation of a solution purification and enantiomeric separation. The lumen side contains an acidic extractor selective to the racemic compounds. The extracted solution is feed into the crystallizer where it contains a chiral selector that will form a salt with the (*S*)-enantiomer and precipitate as a crystal. Adapted from ref. 127.

From a Green Chemistry perspective, more studies must be performed using supported liquid membranes focusing on more environmentally friendly conditions. The used organic solvents must preferably present low toxic potential (**P3**). The more concentrated solutions, the less waste is generated (**P1**) and it is certainly recommended the recycling the used solvents and chiral hosts.

The strategy of Svang-Ariyaskul *et al.* is very interesting because it uses concepts of crystallization and membrane separation in a very innovative way. A good advantage of this process is that there is no need for the addition of a chiral host but only seeds of the enantiomers. The advantage of not using a chiral host is that the purification procedure is simpler because it is not necessary separating the host of the enantiomer, which would require more solvents, reagents, unit operations and energy expenditure (**P1**, **P6**).

The use of an enzyme-mediated resolution process using supported liquid membranes seems a promiscing field and good results were achieved. This approach relies on transformations that make use of natural compounds as reagents under mild conditions. Moreover, enzymes have proven to be more regioselective (**P5**, **P9**).[19]

3.2. Solid membranes for chiral resolution

Solid membranes with inherent chiral chain. There are different approaches to preparing solid membranes from a variety of polymers. Commonly, inherent chiral membranes are prepared by formulating membrane-forming solutions of chiral polymers.[97] The chiral polymers include those that have chiral carbons in the main chain as poly(-γ-methyl-(L)-glutamate),[142–144] alginate,[145] chitosan,[146] cellulose,[147] and their derivatives.[100,148] In 1995, Aoki *et al.*[142] prepared modified poly-(γ-methyl-(L)-glutamate), PMLG, by an ester exchange reaction. Optical resolution of (D)-tryptophan was achieved by pressure-driven permeation through the membrane. The maximum enantioselectivity obtained was 16% of enantiomeric excess. The authors studied the effect of the α-helix content of the membranes and concluded that it did not have a significant effect on the enantioselectivity and permeation rate. Thus, the enantioselectivity of the membrane is resumed to the chiral carbons of the main chain rather than to the conformation of the membrane materials. Thoelen *et al.*[143] also prepared modified PMLG and demonstrated how electrodialysis can be suitable for the resolution of racemic tryptophan with no decrease of enantioselective recognition over time.

Taki *et al.*[144] tested the enantioseparation of racemic tryptophan with poly-(L)-glutamic acid (PLGA) crosslinked with polyetherdiisocyanate membranes immersed in aqueous ethanol. (D)-Tryptophan was selectively transported with a maximum separation factor of 2.6. Kim *et al.*[145] also carried on the resolution of tryptophan, the authors prepared sodium alginate crosslinked with glutaraldehyde membranes. The degree of crosslinking and its effect on enantioselectivity was studied and the outcome was that the less crosslinking, a higher swelling index is obtained, the flux increases but the enantiomeric excess decreases. Therefore, a higher membrane swelling was unfavorable for good optical resolution. A maximum enantiomeric excess of 54% was obtained from a membrane with a swelling index of 80%.

Later, the same co-authors prepared an enantioselective membrane of chitosan for the separation of racemic tryptophan having obtained 98% of enantiomeric excess with a swelling index of 79%.[146] Aoki *et al.*[149] synthesized nine chiral phenylacetylenes containing pinanyl groups and investigated the introduction of chirality in the main chain and formation of chiral helical backbone during polymerization, and its enantioselectivity in the permeation of the polymeric membranes. Results showed that by using the membrane made of poly-[dimethyl(10-pinanyl) silyl] phenylacetylene, (poly-PSPA), the maximum enantiomeric excess was obtained for phenylalanine, valine, and tryptophan were 53.4%, 28.2%, and 99.9% respectively.

Hazarika *et al.*[150] synthesized a polymeric membrane of 1,2-bis(2-methyl-1-triethylsiloxy-1-propenyloxy) ethane and investi-

Open Access Article. Published on 20 May 2022. Downloaded on 14/09/2025 22:14:34.
This article is licensed under a Creative Commons Attribution-NonCommercial 3.0 Unported Licence.

Table 6 A summary of enantioseparation case studies using solid membranes with inherent chiral chain

Material	Product	ee and/or α	Ref.
Poly(L)-glutamic acid	(D)-Tryptophan	α: 2.60	144
Poly(γ-methyl-(L)-glutamate) derivatives	(D)-Tryptophan	16%	142
	(D)-Tryptophan	20% (α: 3.00)	143
Sodium alginate	(D)-Tryptophan	54%	145
Chitosan	Tryptophan	98%	146
Poly[*p*-(oligopinanyl-siloxanyl)phenylacetylene]	Phenylalanine	53.4%	149
	Valine	31.5%	
	Tryptophan	99.9%	
1,2-Bis(2-methyl-1-triethylsiloxy-1-propenyloxy)ethane	*S-trans*-Sobrerol	98.59%	150
Cellulose acetate	2-Phenyl-1-propanol	98%	147
Cellulose	(D)-Mandelic acid	90%	151
	(D)-Mandelic acid	89.1%	152

gated the optical resolution of racemic *trans*-sobrerol by pressure-driven permeation through the membrane. The highest enantiomeric excess was obtained as 98.59% for (*S*)-*trans*-sobrerol using NMP as process solvent.

Xie *et al.*[147] reported the preparation of a cellulose acetate butyrate membrane for the separation of racemic 2-phenyl-1-propanol and enantiomeric excess of up to 98% was achieved.

Ma *et al.*[151] prepared a cellulose membrane and studied the effect of cellulose concentration, drying time, operating pressure, and feed concentration in the membrane properties and its enantioselectivity for (D)-mandelic acid. The maximum obtained enantiomeric excess was 90%. A cellulose membrane was also used by Yuan *et al.*[152] for the resolution of racemic mandelic acid having obtained the enantiomeric excess of 89.1% for the (D)-enantiomer – Table 6.

The end-life management of membrane modules is a great concern. According to the principles of Green Chemistry, the raw material should be renewable rather than depleting (**P7**), thus the membrane material should be selected accordingly. Chitosan, Cellulose, PLGA and sodium alginate are renewable feedstocks and presented good results as it can be seen in Table 6.

Composite membranes. High porous materials that are inherently chiral might offer both high permeability and high selectivity. However, the combination of these desirable features is rare. Likewise, an ideal enantioselective membrane should be relatively simple to synthesize and have satisfactory mechanical properties.[153] Composite membranes consist of a bi-layer film: a porous support layer and a superficial thin dense layer that can be enantioselective.[154] Therefore, composite membrane offers an excellent combination of selectivity, permeability, and mechanical stability.

In 2011, Ingole *et al.*[155] reported the chiral separation of racemic lysine and arginine through enantioselective polysulfone membranes containing a superficial layer of chiral metal–Schiff base complexes. The same co-workers described the resolution of racemic arginine using *trans*-1,4-diaminocyclohexane as the chiral selector (ee: 92%)[156] and the resolution of lysine and asparagine using (L)-arginine as the chiral selector (ee: 91.6 and 67.8% respectively).[157] Devi *et al.*[158] reported the optical resolution of racemic mixtures of arginine and alanine. The chiral selective layer of the membrane was prepared by interfacial polymerization of metaphenylenediamine, trimesoyl chloride, and (*S*)-2-acetoxypropionyl chloride *in situ* on the top of polysulfone membrane (Table 7).

Miao *et al.*[159] described the chiral resolution of tryptophan by using a modified polysulfone membrane prepared *via* mussel chemistry. The membranes were modified with dopa-

Table 7 Overview of enantioseparation case studies using composite membranes

Support layer	Superficial layer	Chiral selector	Product	ee or α	Ref.
Polysulfone	TMC in hexane	Metal Schiff complex	Lysine	94%	155
			Arginine	84%	
Polysulfone	TMC in hexane	*trans*-1,4-Diaminocyclohexane	Arginine	92%	156
Polysulfone	TMC in hexane	(L)-Arginine	Lysine	91.6%	157
			Asparagine	67.8%	
Polysulfone	*meta*-Phenylenediamine, TMC in hexane	(*S*)-2-Acetoxypropionyl chloride	Arginine	92%	158
			Alanine	68%	
Polysulfone	Polydopamine	Ethylenediamine-β-cyclodextrin	Tryptophan	3.2%	159
PE/PP + polyamide nanofiber (PA6)	MPD/DACH in aqueous phase, TMC in hexane	DACH	Tryptophan	45%	160
Polysulfone	*m*-Phenylene-diamine, TMC in hexane	α-Cyclodextrin	Tryptophan	1.55	161
Polysulfone	Carbon nanotubes	(D)-Tryptophan	Tyrosine	98.86%	162
Cellulose acetate	TMC	Ethylenediamine-β-cyclodextrin	Warfarin	9.29%	163
			Ibuprofen	3.77%	
			Tryptophan	27.2%	

Open Access Article. Published on 20 May 2022. Downloaded on 14/09/2025 22:14:34.
This article is licensed under a Creative Commons Attribution-NonCommercial 3.0 Unported Licence.

mine, and β-cyclodextrin as a chiral selector. Gaálová *et al.*[160] prepared a composite membrane from a polyethylene/polypropylene and polyamide nanofiber. The authors prepared a thin, selective layer by interfacial polymerization of two immiscible phases on the porous nanofiber layer: *m*-phenylene diamine (MPD) and (*S*,*S*)-1,2-diaminocyclohexane (DACH) were dissolved in water while 1,3,5-trimesoyl chloride (TMC) was dissolved in *n*-hexane; the active film was obtained by remittent immersion of the fibrous composite in both phases and subsequent thermal treatment.

Zhou *et al.*[161] reported the synthesis of modified polysulfone membrane with a superficial thin layer containing α-CD as the chiral selector and MPD monomer for interfacial polymerization. (L)-Tryptophan was obtained with a separation factor of 1.55 by a concentration gradient mode.

Gogoi *et al.*[162] demonstrated how single-walled carbon nanotubes can be used to increase the hydrophilicity, mechanical strength, and thermal stability of the membrane. The prepared membrane was applied for the separation of (D/L)-tyrosine having obtained 98.86% of enantiomeric excess for (D)-tyrosine.

Ke *et al.*[163] reported a novel chiral thin-film composite polyamide membrane that was fabricated by using *in situ* interfacial polymerization. Ethylene-beta-cyclodextrin (EDA-β-CD) was the chosen chiral selector and it was polymerized with TMC to form a thin layer at the surface of a commercial cellulose acetate membrane.

Graphene oxide membranes. In recent years, graphene and its derivatives (*e.g.*, graphene oxide (GO)) have emerged as nano-building blocks for separation membranes because of the atomic thickness, mechanical strength, thermal stability, and chemical inertness.[164,165] Notably, GO functionalized with chiral selectors has been confirmed to possess exceptional enantioselective performances toward enantiomeric target compounds.

Meng *et al.*[166] integrated a chiral selector (L)-glutamic acid into GO flake *via* a simple vacuum filtration method. Enantioseparation performances were studied of amino acid modified GO membranes toward 3,4-dihydroxy-(D/L)-phenylalanine with a separation factor of 2.05. The results demonstrated how modified GO membranes might provide enantioseparation by enabling high-flux and high-selectivity.

The same co-authors prepared GO-based composite membranes *via* tuning the interlayer spacing between the GO-sheets using PLGA. The incorporated PLGA would not only serve as an additional chiral selector, facilitating the transport of (D)-enantiomer of the chiral probe, but also as a kind of filler, reducing the size of pores or channels between GO sheets. The separation factor obtained was 2.80 for 3,4-dihydroxy-(D)-phenylalanine (Table 8).[167]

Qie *et al.*[168] prepared nanoporous graphene oxides covalently functionalized with β-cyclodextrin as chiral selector. (L)-Asparagine was obtained with great enantioselectivity with more than 99% of enantiomeric excess.

Meng *et al.*[169] proposed a new strategy to improve the enantioseparation performances of GO membranes by controlling the degree of functionalization with an epoxide ring-opening reaction with a carboxyl-terminated ionic liquid as a spacer and an active site for the chiral selectors, followed by an amidation reaction of (L)-glutamic acid as chiral selectors. The authors concluded that these membranes are superior in the enantioselectivity and 1–3 orders of magnitude higher in the flux than traditional chiral separation membranes. The separation factor obtained was 3.89 for 3,4-dihydroxy-(D)-phenylalanine.

Recently, the same co-workers[170] prepared an (L)-phenylalanine modified GO-based membranes, and its enantioselectivity was tested for racemic phenylalanine, methionine, *N*′-acyl-phenylalanine, and *N*′-acyl-methionine. Results showed that the prepared membrane presented stronger interaction toward (D)-enantiomers essentially caused by the additional non-stereoselective component between GO surfaces and chiral probes.

Carbon nanomaterials play an important role in resolving the increasingly urgent energy and environmental crises due to their intrinsic chemical and mechanical properties. However, the harmful environmental impacts on their preparation might reduce the sustainability (**P3**). Therefore, new technologies for carbon nanomaterials preparation must be developed to minimize environmental impacts.[171]

Chiral microporous membranes. Recently, chiral microporous material has attracted much attention for continuous chiral separation due to their well-defined homochiral pores, great potential in adsorption/storage, specific surface area, and versatile chemical functionalities as compared to other materials.[172–174] It can be used as coated tubular columns for high-resolution GC or HPLC[175–177] Moreover, they can be classified as MOFs, hydrogen-bonded organic frameworks (HOFs), and covalent organic frameworks (COFs).[178–185]

Table 8 Summary of enantiomeric resolution using graphene oxide membranes

Chiral selector	Product	ee or α	Ref.
(L)-Glutamic acid	3,4-Dihydroxy-(D)-phenylalanine	2.05	166
PLGA	3,4-Dihydroxy-(D)-phenylalanine	2.80	167
β-Cyclodextrin (β-CD)	(L)-Asparagine	99%	168
(L)-Glutamic acid-functionalized with an ionic liquid	3,4-Dihydroxy-(D)-phenylalanine	3.83	169
(L)-Phenylalanine	(D)-Phenylalanine	1.72	170
	(D)-Methionine	1.10	
	N′-Acyl-(D)-phenylalanine	1.80	
	N′-Acyl-(D)-methionine	1.30	

Open Access Article. Published on 20 May 2022. Downloaded on 14/09/2025 22:14:34.
This article is licensed under a Creative Commons Attribution-NonCommercial 3.0 Unported Licence.

MOFs are a family of porous crystalline materials constructed with coordinate bonds between inorganic secondary building units and organic ligands.[179,186] HOFs have some advantages such as easy purification, straightforward regeneration, and re-usability by simple recrystallization.[187] This type of membrane presents high enantioselectivity because of its porous chiral channels and consequently high permeation flux and low mass transfer resistance.[188] Moreover, enantiomer separation can be optimized by tuning the pore size or shape and introducing a chiral functional group into a MOF.[176] Also, the use of mixed matrix membranes (MMMs) that combine the advantages of a polymeric matrix and the molecular selectivity of microporous materials can provide a simpler approach to achieve enhanced permeability and selectivity.[101,189]

A few MOFs and their derivative membranes for chiral separation have been reported recently. Also, coupling chiral ligands to the MOFs has been applied to tune the chirality of achiral MOFs for asymmetric catalysis.[190–193]

Kepert *et al.*[194] reported that the stereochemistry of alcohol templates spontaneously resolves to form homochiral helical structures featuring helical networks. Therefore, the enantioselective adsorption property was successfully established for the first time by the homochiral MOFs.

In 2011, the resolution of 2,5-hexanediol was performed under continuous flow mode by Liu *et al.*[195] The authors selected surface-mounted metal–organic frameworks to study the adsorption of (*R*/*S*)-hexanediol from the gas phase (vapor) in a continuous-flow mode using nitrogen gas as a carrier.

In 2012, a homochiral MOF membrane [Zn_2(bdc)((L)-lac)(dmf)] was prepared for the enantioselective separation of (*S*)-methyl phenyl sulfoxide that can be used as synthetic auxiliary and valuable pharmaceutical.[188]

In the following year, Kang *et al.*[196,197] developed a method named "Single nickel source" for *in situ* fabrication of a high thermal stable homochiral MOF. A diol isomer mixture was used to test the separation efficiency of the membrane at different temperatures and pressures obtaining ee of 32.5% (Table 9).

In 2014, Li *et al.*[187] prepared a homochiral microporous hydrogen-bonded organic framework (HOF-2) based on a BINOL derivative that has been synthesized and structurally characterized, presenting permanent porosity and highly

Table 9 Overview of enantioseparation case studies using chiral microporous membranes

Framework	Ligand	Enantiomer	ee%	Ref.
[Zn_2(bdc)((L)-lac)(dmf)]	1,4-Benzenedicarboxylate (bdc) (L)-Lactic acid ((L)-lac)	(*S*)-Methyl phenyl sulfoxide	20	188
Ni_2((L)-asp)$_2$(bipy)	4,40-Bipyridine(bipy)	2-Methyl-2,4-pentanediol	32.5	196 and 197
HOF-2	(*R*)-1,10-Bi-2-naphthol scaffold into 2,4-diaminotriazinyl	1-Phenylethanol	92	187
		1-(4-Chlorophenyl)ethanol	79	
		1-(3-chlorophenyl)ethanol		
		2-Butanol 2-pentanol 2-hexanol	66	
		2-Heptanol	77	
			48	
			<10	
			<4	
(*S*)-[DyNaL(H_2O)$_4$]	3,30-Di-*tert*-butyl-5,50-di (3,5-carboxyphenyl-1-yl)-6,60-dimethylbipheny(L)-2,20-diol ligand (H_4L)	(L)-Methyl mandelate ethyl mandelate i-propyl mandelate	93.1	207
		(D)-Methyl mandelate benzyl mandelate	64.3	
			90.7	
			89.9	
			73.5	
(D)-His-ZIF-8	(D)-Histidine	Alanine	78.52	199
		Glutamic acid	79.44	
[Co_2(*S*-man)$_2$(bpy)$_3$](NO_3)$_2$·guest	Mandelate and 4,4′-bipyridine	1-Phenyl-1-propanol	60	200
(L)-His-ZIF-8	(L)-Histidine	1-Phenylethanol	76	204
H-(D)-his-ZIF-8	(D)-Histidine	Alanine	90.5	205
		Glutamic acid	95.2	
		lysine	92.6	
[Cd_2(CO_2)$_4$(DMF)$_2$(H_2O)]	1,1′-Biphenol	1-Phenylethanol	99	206
		1-Phenylpropanol	92	
		1-(1-Naphthyl)ethanol	99.4	
		1-(4-Fluorophenyl)ethanol	93	
		1-(4-Chlorophenyl)ethanol	98	
		1-(4-Bromophenyl)ethanol	98	
		Methyl phenyl sulfoxide	83	
		Ethyl phenyl sulfoxide	80	
		3-Methoxy phenyl methyl sulfoxide	96	
		Lansoprazole	91	
MIL-53-NH_2/PES MMM	(L)-Histidine (L)-Glutamic acid	1-Phenylethanol	100	189
γ-CD-MOF/PES MMM	γ-Cyclodextrin	1-Phenylethanol	100	101

Open Access Article. Published on 20 May 2022. Downloaded on 14/09/2025 22:14:34.
This article is licensed under a Creative Commons Attribution-NonCommercial 3.0 Unported Licence.

enantioselective separation of chiral secondary alcohols with ee value up to 92% for 1-phenylethanol. Based on the work of Brunet *et al.*,[198] they showed that 2,4-diaminotriazinyl is a very powerful hydrogen-bonding backbone for the construction of porous robust HOFs, and the use of highly enantioselective separation of small molecules.

In 2015, Zhao *et al.*[199] prepared a microporous MOF structure, with a chiral environment using (D)-histidine as chiral ligand, (D)-his-ZIF-8. The membrane shows selective separation capability for racemic alanine and glutamic acid, with an ee value of 78.5% and 79.4% respectively.

Zhang *et al.*[200] reported a single-step synthesis of MOFs based upon mandelate (man) and 4,4′-bypyridine ligands and enantioselective recognition toward the (*R*) enantiomer of 1-phenyl-1-propanol was observed with ee values of up to 60%.

In 2017, Liu *et al.*[201,202] demonstrated a superficial chiral etching process to introduce chiral function on achiral MOF surface for enantioselective adsorption toward limonene enantiomers. In the following year, the co-workers[203] prepared a MOF–chiral polymer composite, which integrates chirality, porosity, and conductivity into the composite for enantioselective adsorption and sensing for carvone enantiomers.

Chan *et al.*[204] prepared (L)-his-ZIF-8 that exhibited good selectivity for the (*R*)-enantiomer of 1-phenylethanol over the (*S*)-enantiomer, showing a high ee value up to 76%. Wang *et al.*[205] prepared chiral ZIF-8 hollow nanospheres with (D)-histidine as ligand. Due to the higher surface area and consequently more accessible chiral groups, the hollow cavity can be more attractive for guest-sorption.

Abbas *et al.*[206] described a chiral porous 3D MOF built from an enantiopure carboxylate ligand of 1,1′-biphenol, which can be utilized as an adsorbent for the separation of aromatic alcohols and sulfoxides with enantioselectivity of up to 99.4%.

In 2019, Wang *et al.*[208] reported a facile and scalable approach: a thermally induced phase separation-hot pressing to fabricate flexible membranes with ultrahigh MOF loading (up to 86 wt%) for separation applications. The membranes presented good mechanical behavior, hierarchical porous structure, and large surface area. High flux, and rejection rate for water treatment with the ability to catch small molecules under crossflow filtration mode.

Lu *et al.*[189] described a new type of enantioselective MMM derived from homochiral MIL-53 nanocrystals with polyethersulfone as a polymeric matrix and aminoacids as chiral ligands. And recently the authors reported γ-CD-MOF-based MMMs with polyethersulfone as a matrix for efficient separation of racemic 1-phenylethanol.[101] More information about the preparation and applications of cyclodextrin-MOF can be found in the reviews.[209–212]

Chen *et al.*[213] described the preparation of a three-dimensional hierarchically porous organic/inorganic composite by incorporation of the hyper-cross-linked resin organic polymer with macroporous silica gel sheet, followed by a chiral selector post-modification. Racemic 1-phenylethanol, ibuprofen, and naproxen could be separated successfully with complete resolution.

Molecularly imprinted membranes (MIM). Enantiomers separation challenges may not be solved with existing commercial membranes since the success of the resolution depends on the recognition of the desired enantiomer functional groups with the membrane backbone.[98] Molecular imprinting is a promising field in which a polymer network is prepared with specific recognition for the desired template molecule.

In a classical approach, it is needed a template, a functional monomer, a cross-linker, a polymerization initiator, and a solvent.[214] The functional monomers will be designed to interact with the template *via* covalent or non-covalent bonding.[215] Furthermore, the monomers are polymerized in the presence of the template that afterward will be removed. The resulting membrane will have specific binding sites to the compound of interest. MIMs may be used on a large scale due to their obvious advantages including ease of preparation, scalability, stability, and low material cost.[216] Interesting reviews about the application of molecularly imprinted membranes can be found in the literature.[98,214,215,217–220]

The first application of molecularly imprinted membrane was developed by Michael's research group in 1962.[221] They prepared polyethylene membranes imprinted with *p*-xylene that were able to selective transport *p*-xylene over the corresponding isomers, *ortho* or *m*-xylene. In 1972, Wulff and co-workers developed a methodology for the introduction of molecular recognition sites into a polymeric matrix in a specific steric arrangement.[222–224]

Enantioseparation using MIM has been intensively studied by using alternative molecular imprinting, a technique that can convert any polymeric material into an enantioseparation membrane.[225–233] In general, it is necessary to employ the optically pure print molecule to obtain MIM for chiral recognition and separation.[219] The chiral recognition ability was found to be dependent on the absolute configurations of both the print molecule and the amino acid oligopeptide residues. Specifically, a membrane consisting of oligopeptide residues from a (D)-amino acid and imprinted with a (D)-amino acid derivative recognized the (D)-enantiomer in preference to the corresponding (L)-enantiomer and *vice versa*.[220]

Since 1995, Yoshikawa and co-workers published a considerable amount of work based on molecularly imprinted membranes for enantiomers resolution. The authors explored molecularly imprinted nanofiber and polymeric membranes prepared from carboxylated polysulfone, polysulfone-aldehyde, myrtenal-containing polysulfones, cellulose acetate, novel polyurea membranes synthesized from lysinyl residues, polyamide, tri, and tetrapeptide derivatives, and *N*-α-benzyloxycarbonyl-(D/L)-glutamic acid (Boc-(D/L)-Glu) and *N*-α-benzyloxycarbonyl-(D/L)-tryptophan (Boc-(D/L)-Trp) as templates. They determined separation factors for tryptophan enantiomers and their derivatives,[227,230–237] glutamic acid,[225,226,228,238–244,245] and other aminoacids (Table 10).[229,246]

The co-workers also studied how the number of constituent amino acid residues influence the molecular recognition ability of the membrane (tri and tetrapeptide derivatives) and it was concluded that the tetrapeptide derivative was the best

Open Access Article. Published on 20 May 2022. Downloaded on 14/09/2025 22:14:34.
This article is licensed under a Creative Commons Attribution-NonCommercial 3.0 Unported Licence.

Table 10 Summary of chiral resolution using molecularly imprinted membranes

Mode	Framework	Imprinted molecule	Enantiomer	ee or α	Ref.
Electrodialysis	Polysulfone	(L)-Phe	(L)-Phenyl-alanine	4.10	255
	Polystyrene resin + tetrapeptide derivative (Boc-DIDE-resin)	(L)-Trp	(D)-Tryptophan	1.40	234
	Nylon-6	(L)-Glutamine	(L)-Glutamine	1.0	248
	Tetrapeptide derivative	Boc-(L)-Trp	*N*′-α-Acetyl-(L)-tryptophan	6	236
	Polystyrene resin			6	232
	Tripeptide derivative			4.5	233
	Aminomethylated polystyrene resin + oligopeptide tweezers			2.5	235
	Tetrapeptide derivative	Boc-(D)-Trp	(D)-Tryptophan	1.0	229
			(D)-Phenylalanine	1.0	
			(D)-Alanine	1.0	
	Tetrapeptide derivative	Boc-(L)-Trp	(L)-Arginine	1.3	246
			(L)-Lysine	1.3	
			(L)-Histidine	1.4	
			(L)-Asparagine	1.2	
			(L)-Glutamic acid	1.3	
Electro-dialysis	Cellulose acetate	Boc-(D)-Glu	(D)-Glutamic acid	2.30	244
Pressure driven	Cellulose acetate		(D)-Glutamic acid	1.45	243
Electrodialysis	Myrtena(L)-containing polysulfones	Boc-(L)-Glu	(L)-Glutamic acid	1.59	228
	Chiral polyurea			1.14	239–242
	Polysulfone-aldehyde derivatized			1.25	245
Conc. driven	Chitosan/GPTMS	(L)-Phenylalanine	(D)-Phenylalanine	4.5	249
Temp. driven	Poly-(methyl methacrylate)-*N*-isopropyl acrylamide (PMMA-PNIPAm)	(*R*)-Equol	(*S*)-Equol	2.60	252
Conc. and pressure	Chloromethylated polysulfone (CMPSF) + dimethylaminoethyl methacrylate (DMAEMA), *N*,*N*′-methylene-bisacrylamide (MBA)	(L)-Aspartic acid	(L)-Aspartic acid	82% (7.52)	253
Pressure driven	Alumina template with ZrO_2 + cellulose acetate	(L)-Mandelic acid	(D)-Mandelic acid	94.5% (35)	254

candidate for forming molecular recognition sites. Moreover, it was interesting to identify those membranes that were imprinted with an amino acid with a certain configuration, recognizing not only the target amino acid but also analogs that had the same absolute configuration.

Electrodialysis was recognized as a suitable driving force for membrane enantioselective transport. In 1999, Dzgoev and Haupt prepared molecularly imprinted polypropylene membranes with Boc-(L)-tyrosine as a template. The results confirmed that the imprinted molecule recognizes the compounds with the same absolute configuration, in this case, Boc-(L)-tyrosine.[247]

Screenivasulu Reddy *et al.*[248] functionalized Nylon-6 by alternative molecularly imprinted membrane technique with (L)-glutamine. The authors acknowledged that the binding of (L)-glutamine increased with the increase of the amino acid concentration. A maximum separation factor of 1 was obtained. Jiang *et al.*[249] prepared an enantioselective MIM using chitosan as bulk polymer, (L)-phenylalanine as imprinting molecules, and γ-glycidoxypropyltrimethoxysilane as the crosslinking agent. Significantly selectivity with a separation factor of 4.5 for (D)-phenylalanine was achieved.

Molecularly imprinted composite membranes were prepared by Son and Jegal.[250] They used polysulfone as a support layer, piperazine and TMC in hexane as a superficial layer, and (D)-serine as a chiral template. The membrane proved to be effective for the selective permeation of (D)-serine having obtained a maximum enantiomeric excess of 80%. Also, Bing *et al.*[251] developed PVDF hollow-fiber membranes modified by a thin layer of a molecularly imprinted polymer prepared with levofloxacin, methacrylic acid, and ethylene glycol dimethacrylate that allowed selective separation of levofloxacin.

Lei *et al.*[252] prepared a molecularly imprinted cation-exchange membrane for the resolution of racemic Equol. The membrane preparation resumed to a one-pot approach to obtain monodispersed methyl methacrylate-*N*-isopropyl acrylamide polymer by atom transfer radical precipitation polymerization. The maximum obtained separation factor was 2.60.

Gao *et al.*[253] used a chloromethylated polysulfone membrane and applied an advanced surface imprinting technique for the separation of a racemic mixture of aspartic acid. By amine modification, an aminated polysulfone membrane was obtained. The imprinting layer was attained from dimethylaminoethyl methacrylate as functional monomer, *N*,*N*′-methylene-bisacrylamide as the crosslinking agent, $(NH_4)_2S_2O_8$ as an initiator, and (L)-aspartic acid as a template. A separation factor of 7.52 was obtained for (L)-aspartic acid with an enantiomeric excess of 82%.

Li *et al.*[254] prepared an alumina template modified with ZrO_2 coated with cellulose acetate containing imprinted molecules for a novel enantioselective membrane. (*S*)-Mandelic acid was used as a chiral template. The co-workers studied the impact of changing the concentration of cellulose acetate, and the procedure of molecular imprinting in the morphology and particle size of the ZrO_2-modified Al_2O_3 membrane. The obtained separation factor was as high as 35 for (*S*)-mandelic acid with an enantiomeric excess of 94.5%.

Open Access Article. Published on 20 May 2022. Downloaded on 14/09/2025 22:14:34.
This article is licensed under a Creative Commons Attribution-NonCommercial 3.0 Unported Licence.

Based on the described studies, it seems that complete *enantio*-separation of a racemic mixture through one cycle process with a molecularly imprinted membrane is not feasible. As far as we know, 100% ee cannot be achieved by a single operation. Multi-cycle operation processes might be the path to achieve better separation.[217]

Many advances in synthetic approaches have been made in the last years, however, molecular imprinting methodology still uses high quantities of solvents and intensive process steps.[256]

Computational modeling might be used in the selection of reagents required for the synthesis of MIMs. It can be very useful to avoid unnecessary screening reactions and waste formation (**P1**). The monomers required for the membrane skeleton are selected computationally based on their ability to interact with the template molecule. Similarly, the used solvent can also be selected using computational tools. This results in a careful selection of the necessary reagents to prepare the desired MIM with no generation of waste.[257]

Reusability is a great advantage of MIMs as they can be used continually after a regeneration step. Recycling allows the reduction of reagents that would be required for the preparation procedure. In several studies, MIMs have been repeatedly applied many times with minimum loss in their extraction efficiency (**P1**).[257]

Commonly, the template removal from the MIMs is performed through exhaustive washing with organic solvents. Subsequently, the organic solvents are discarded into the environment.[258] To employ greener methods of template removal, supercritical solvents might be used to replace the organic solvents. Furthermore, the ability to reuse MIMs in many applications reduces the solid waste in the environment.[257]

Sustainability considerations. The development of membrane separation processes has been significant in the last few years. Several unit operations have been redesigned as membrane units.[259] With their intrinsic characteristics of energy efficiency and operational simplicity, it allows a higher selectivity and permeability for the transport of specific components. Additionally, it offers increased compatibility between different membrane operations in integrated systems, low energetic requirement, good stability under operating conditions and environmental compatibility, easy control, and scale-up.

Our planet is facing environmental pollution and a serious energy crisis. A green mindset may offer important help to overcome these challenges. The green chemistry principles encourage the use of safer solvents and processes with lower impact on the environment by preventing waste and increasing energy efficiency. Membrane technology is considered a green and sustainable technology because of its relatively low energy consumption.[260] Nevertheless, traditional membrane fabrication methods negatively affect sustainability.[261] As described in this review, membranes should offer a good transport rate with high selectivity, be stable in a high range of pH, compatible with different types of solvents, superior antifouling properties, and minimal aging or swelling.[261]

Membrane fabrication frequently employs non-environmentally friendly solvents as NMP, DMF, and DMAC. These traditional procedures must be absolutely substituted by manufacturing processes that make use of green solvents.[261]

Certainly, green solvents might provide a similar membrane performance when compared to the traditional ones, however, the manufacturing processes are still costly. In fact, due to the inherent advantages compared to the greener alternatives, namely reproducibility in large scales, increased solubility, and lower cost, classical solvents have been preferred. Fortunately, some researches indicate that it is completely possible to achieve these goals with greener solvents, not yet now but very soon.[262] Moreover, the treatment and recycling of the used organic solvents may be a viable approach to reduce waste.

The end-life management of membrane modules is another great matter. The reuse of membrane tools rather than their direct incineration should be encouraged to drive membrane technology to a greener level.[261]

4. Continuous chromatography

4.1. Simulated moving bed chromatography

The conventional four-zone simulated moving bed (SMB) chromatography unit consists of a closed system with several packed columns connected in a loop. The system is divided into four zones by two inlets named feed and eluent/desorbent and two outlets named extract and raffinate.

A racemic solution feed is continuously fed into the process through the feed stream, and an eluent solution (usually the same solvent composition as feed solution) is fed into the process through the eluent stream. The enantioseparation occurs in the packed columns containing a chiral stationary phase and the solutions are collected at two outlets (raffinate: less retained enantiomer, extract: more retained enantiomer). The remaining mixture of enantiomers that has not been separated can be recycled through the columns while the feed racemic solution is feed.[263] A SMB process does not reach the steady-state but the cyclic steady state because of the periodic repetition of port switching.[263] The key advantages of an SMB process over batch chromatography is the cost-effective potential to enhance productivities and to reduce the solvent consumption compared to conventional discontinuous processes.[264,265]

The first application of a countercurrent SMB chromatography was described in Broughton's patent from 1961 and was widely adopted in the petrochemical industry and for complex separations.[266] In 1992, the application of SMB for enantioseparation was reported for the resolution of 1-phenylethanol.[267] Negawa and Shoji used an eight-column SMB unit packed with Chiralcel OD and a mixture of hexane and isopropanol as eluent and developed a purification process with great advantages when compared to the batch process, namely a minor solvent consumption by using more concentrated solutions and increased productivity since it is performed in

Open Access Article. Published on 20 May 2022. Downloaded on 14/09/2025 22:14:34.
This article is licensed under a Creative Commons Attribution-NonCommercial 3.0 Unported Licence.

continuous mode. Since then, several patents about enantioseparation of active pharmaceutical ingredients and their analogs were published, namely for (*S*)-levetiracetam,[268] sertraline,[269] oxetine,[270] pharmaceutically desired chiral tetralones,[271] and Schiff bases.[272] Diehl *et al.*[273] developed the resolution of *cis*-8-benzyl-7,9-dioxo-2,8-diazabicyclo[4.3.0] nonane, a quinolone derivative by SMB chromatography in a kilogram scale with enantiomeric excesses above 98%.

In 1993, Ching *et al.*[274] published the continuous purification of racemic Praziquantel, an anthelminthic API, by SMB chromatography with a four-column configuration. The coauthors optimized the process[275,276] having obtained maximum purity of 97.5% for the (L)-enantiomer and from the obtained raffinate solution, it was possible to concentrate it and crystallize the desired enantiomer with an overall yield of 80%. In 2016, Andrade Neto *et al.*[277] reported a theoretical study about adaptive nonlinear model predictive control (NMPC) strategies to separate racemic praziquantel using SMB chromatography. Finally, in 2019, Cunha *et al.*[278] described the resolution of praziquantel with an SMB built-in-house unit with [1-2-2-1] column configuration with 100% chiral purity for the (L)-enantiomer (Table 11).

In 2000, Ludemann-Hombourger *et al.*[279] reported a new model of a continuous chromatographic process called "Varicol" based on a non-synchronous shift of the inlet/outlet valves in a multicolumn system as opposed to the classical SMB process. Consequently, the zone lengths are continuously oscillating by one column, with the increase of one zone being compensated by the decrease of an adjacent one delivering continuous streams without reaching a steady state. The differences concerning the SMB are that: the zone lengths are not constant in time which means the number of columns per zone is not constant, the inlet/outlet lines are not shifted simultaneously, and lastly, there is no constant solid flow rate concerning the inlet/outlet lines. The authors performed the enantioseparation of 1,2,3,4-tetrahydro-1-naphthol and compared the efficiency of both Varicol and SMB approaches. It was used Chiralpak AD packed columns and a mixture of heptane, isopropanol, and trifluoroacetic acid (TFA) 95/5/0.2 (v/v/v) as eluent. By using theoretical and experimental results, the coworkers showed with specific column configurations and solid flow rate, that the performance of a 6-columns SMB can be obtained with a 5-columns Varicol, with this last operation mode presenting higher productivity and solvent consumption.

Several studies on the comparison of operation strategies for enantiomers separation by SMB chromatography have been carried out and demonstrated numerically.[263,280–284] Including temperature gradient,[285] solvent gradient[265,286–288] time variability[289] known as PowerFeed mode and modulation of the feed concentration during the switching cycles (ModiCon).[290] Also, different types of SMB apparatus were patented by Vroon *et al.*[291] and Michel Anton.[292] Zhang *et al.*[281] investigated numerically four different modes of SMB: Varicol, PowerFeed, ModiCon, and classical SMB in three to five column units and compared the obtained results. The authors also considered the possibility of combining two operating modes in a new hybrid process and evaluated the feasibility. The conclusions taken on the studied scenario involving chiral separations, the PowerFeed, and ModiCon modes allow one to achieve even better performance than Varicol and classical SMB.

Lee *et al.*[294,295,304] developed a standing-wave design method for nonlinear simulated moving bed (SMB) systems with significant mass-transfer effects and an operating pressure limit. It was also possible to determine ideal column lengths for process optimization. The enantioseparation of

Table 11 Overview of enantiomeric separation by SMB systems

Product	Chiral stationary phase	Eluent	Purity	Ref.
(*R*)-1-Phenylethanol	Chiralcel OD	Hexane : IPA	99%	267
(*S*)-1-Phenylethanol			92%	
(L)-Praziquantel	Microcrystalline cellulose triacetate	MeOH	93.7%	274
(D)-Praziquantel			90.1%	
(L)-Praziquantel	Microcrystalline cellulose triacetate	MeOH	97.5%	275 and 276
(D)-Praziquantel			85%	
1,2,3,4-Tetrahydro-1-naphthol	Chiralpak AD	Heptane, isopropanol and TFA 95 : 5 : 0.2	98%	279
(*S*)-Levetiracetam	Chiralpak AD	EtOH : ciclohexane	98%	268
(*S*)-Ketoprofen	Kromasil TBB	Hexane, MTBE, AcOH (85 : 15 : 0.1)	96%	293
Phenylpropanolamine	Chiralpak AD	MeOH	99%	294 and 295
(*S*)-Pindolol	Chiral-AGP	Water : ACN	99%	296
(*S*)-Ibuprofen	Kromasil TBB	Hexane : TBME : AcOH	100%	297
Guaifenesin	Chiralpak AD	Heptane, EtOH (85 : 15)	98%	298
Quinolone derivatives	Chiralpak AD	Acetonitrile	98.9%	273
(*S*)-Ketoprofen	Chiralpak AD	EtOH : TFA 0.01%	98.6%	299
(*R*)-Ketoprofen			99.8%	
(*R*)-Aminoglutethimide	Chiralcel OD	Hexane : EtOH : ethanolamine	99%	264
(2*R*,3*S*,2*R*)-Nadolol	Chiralpak IA	MeOH : ACN : diethylamine (25 : 75 : 0.1)	100%	300
(L)-Praziquantel	Chiralcel OZ	MeOH	100%	278
(D)-Praziquantel			97%	
(*R*)-Guaifenesin	Chiralcel OD	Hexane : EtOH (70 : 30)	99.0%	301 and 302
(*S*)-Guaifenesin			99.0%	
(2*S*,3*S*)-Butanediol	Chromalite-PCG600M	Water	99%	303 and 304

Open Access Article. Published on 20 May 2022. Downloaded on 14/09/2025 22:14:34.
This article is licensed under a Creative Commons Attribution-NonCommercial 3.0 Unported Licence.

phenylpropanolamine was used to test the design method. Purities of 99% were obtained. The separation of racemic pindolol is of great commercial value because *S*-pindolol is the effective component for the treatment of hypertension.

Zhang *et al.*[296] reported theoretical and experimental investigations of the enantioseparation of racemic pindolol by classical SMB and Varicol approach with a five-column setup. In the first study, the co-workers selected the operating conditions based on a mathematical model, and finally, they validated the model predictions. The chosen eluent was water and acetonitrile (ACN) 90 : 10, respectively. The effect of column configuration was explored and the configuration [1-2-1-1] was superior for the classical SMB approach. For the Varicol approach, a configuration of [1.5-1.5-1-1] was used. The authors also studied the effect of eluent recycling on the product's final purity. In both approaches, 100% purity was obtained.

Park *et al.*[297] separated racemic ibuprofen in an SMB four-column unit and performed experiments based on simulation results from ASPEN chromatography software. The authors studied the effect of feed concentration/flow rate on the final purity of the raffinate stream. Final purities of 100% for (*S*)-ibuprofen (raffinate stream) were obtained. Ketoprofen enantiomers were first separated by SMB chromatography in 2004 by Yoon *et al.*[293] in a six-column (1-2-2-1) configuration packed with Kromasil TBB stationary phase and a mixture of *n*-hexane, methyl-*tert*-butyl ether (MTBE), and acetic acid (AcOH) as eluent. For the same purpose, Ribeiro *et al.*[305] carried on an exploratory study on how eluent composition influences the adsorption behavior of ketoprofen enantiomers in packed Chiralpak AD columns. Later, the same co-workers[299] set up a six-column (1-2-2-1) configuration packed with Chiralpak AD as stationary phase and utilized ethanol with 0.01% trifluoroacetic acid (TFA) as eluent. The maximum obtained productivity was 3.84 g L^{-1} h^{-1} and purities of 98.6% and 99.8% for (*R*)-ketoprofen and (*S*)-ketoprofen, respectively.

Jiang *et al.*[306] theoretically investigated the feasibility of an internal temperature gradient established by a difference between feed and eluent temperatures for the separation of ketoprofen enantiomers based on a built model. The separation of aminoglutethimide enantiomers by a continuous multicolumn chromatographic process was investigated theoretically and experimentally by Lin *et al.*[264] A mathematical model was built to design and optimize the operation conditions, and experiments were run using a five-column Varicol process with the column configuration of (1/1.5/1.5/1) and a classical six-column SMB process with (1-2-2-1) configuration. By using the Varicol approach, the (*R*)-aminoglutethimide enantiomer was obtained with a purity of 99.3% and productivity of 2.45 g L^{-1} h^{-1} (59.1 g L^{-1} d^{-1}). When comparing the enantioseparation performance it was found that the Varicol process has a better performance than the SMB process, with a 20% increase of (*R*)-aminoglutethimide productivity.

Arafah *et al.*[300] carried on the enantioseparation of Nadolol in a pilot SMB unit with a classic (1-2-2-1) configuration. The results obtained were remarkable with 100% purity, 100% yield, and system productivity of 0.77 g L^{-1} h^{-1}.

Guaifenesin is a worldwide prescribed drug for cough and cold labeled as an expectorant. Gomes *et al.*[298] explored the separation of a racemic mixture of guaifenesin onto a chiral stationary phase Chiralpak AD by altering mobile phase solvents and proportions, by modeling and designing an SMB unit. The authors obtained purities up to 98%. Some years later, Gong *et al.*[301] reported the resolution of Guaifenesin racemic mixture with the obtention of both enantiomers with 99% purity. The six-column SMB process with 1-2-2-1 column configuration, divided into four zones by two inlet ports (feed and desorbent) and two outlet ports (raffinate and extract) was performed in countercurrent and by switching the position of the inlet and outlet ports under constant feed composition and flow rate. The (*R*) enantiomer was obtained from the raffinate stream as it had weak adsorption to the stationary phase and the (*S*) enantiomer was obtained from the extract stream.

In a second study,[302] the authors determined the separation performance of the SMB unit in four operation modes (conventional SMB, VariCol, PowerFeed, and ModiCon). When compared with the traditional six-column SMB process and with the same column configuration, the PowerFeed mode improved the productivity by 10.6%, and solvent consumption was reduced by 8.7% but also increased the pressure drop and pressure fluctuations which can limit the application. The VariCol mode with a five-column configuration increased the productivity by 26%. Lastly, the ModiCon mode presented the best results, increasing by 27.5% the productivity and decreasing solvent consumption by 21.7% – Fig. 17.

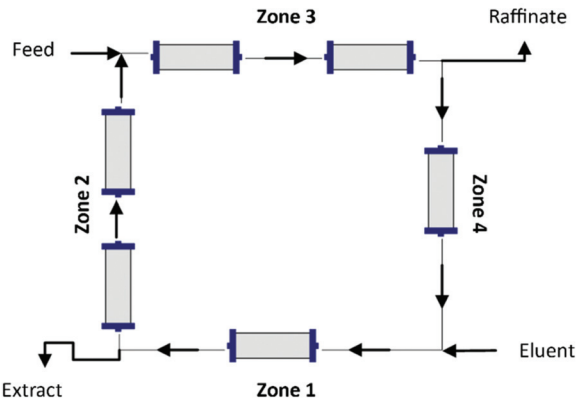

Fig. 17 Set-up for the separation of guaifenesin enantiomers by SMB process with [1-2-2-1] configuration. (feed: racemic solution of guaifenesin; raffinate: solution of (*R*)-guaifenesin; eluent: hexane/ethanol 70/30; extract: *S*-guaifenesin.) Adapted from ref. 301.

The continuous separation of racemic 2,3-butanediol was reported by Lee *et al.*[303,304] In a first study, the adsorption behaviors of the enantiomers in Chromalite-PCG600 M as stationary phase were investigated and numerical computations were carried out in Aspen Chromatography simulator.

Open Access Article. Published on 20 May 2022. Downloaded on 14/09/2025 22:14:34.
This article is licensed under a Creative Commons Attribution-NonCommercial 3.0 Unported Licence.

Both 2,3-butanediol enantiomers could be separated with high purities up to 97% and yield in a continuous countercurrent mode. In a second study, to increase productivity and meet the quality requirements, a simulated process optimization was carried out based on a Langmuir isotherm standing-wave-design method to explore the effects of feed concentration and/or column length on the production rate. The great advantages of using an SMB process are that the purification can be performed in continuous, better product purities and yield can be achieved, and it was not necessary any complementary reactions for product derivatization and isolation.

In 2016, Fuereder *et al.*[307] reported the integration of simulated moving bed chromatography and enzymatic racemization enabling the synthesis of single enantiomers from a racemic mixture is theoretically 100% yield overcoming the limitation of conventional SMB processes by only separating the enantiomers and not racemizing one into the other. The system contained Chirobiotic TAG columns-SMB unit, an amino acid racemase-containing enzyme membrane reactor, and a nanofiltration unit for the concentration of the SMB raffinate stream before racemization on lab-scale to produce enantiopure (D)-methionine. The process was running for 30 h without significant variations in product concentration and purity and with a global yield of 93.5% (Fig. 18).

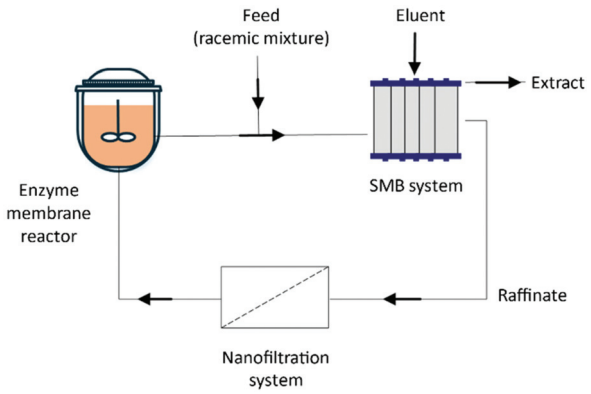

Fig. 18 Integration of simulated moving bed chromatography, enzymatic racemization and nanofiltration to produce (D)-methionine. Extract: (D)-methionine solution; raffinate: (L)-methionine solution; nanofiltration system: concentration of the raffinate solution; enzyme membrane reactor: racemization of (L)-methionine.[307]

Recently, Harriehausen *et al.*[308] reported the synthesis of enantiopure mandelic acid and methionine enantiomers exploiting enzymatic racemization coupled with SMB chromatography. The key idea is to recycle the undesired enantiomer from the SMB process, racemize this recycling solution, and concentrate it in a solvent removal unit. The authors tested two different types of SMB unit configurations (1) a closed-loop four-zone and (2) an open-loop three-zone SMB separation process. The main outcome was that configuration (2) outperformed the conventional (1) setup. The configuration (2) could save 25% of the stationary phase, leading to a productivity enhancement of 33%. Moreover, the co-workers concluded that for the obtention of high productivities it is essential to use highly selective stationary phases, and high feed concentrations, which are limited by solubilities of the compounds in the eluent. Also, the SMB unit should be designed for less retention of the target enantiomer to elute it at the raffinate outlet (Fig. 19).

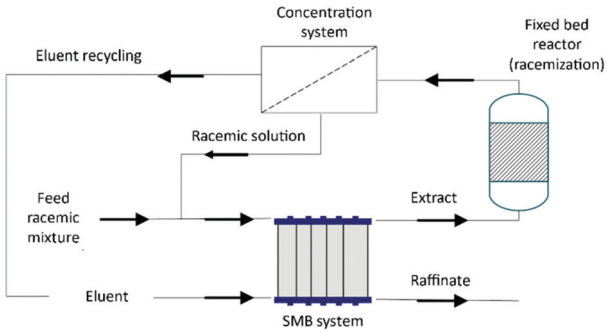

Fig. 19 Integration of simulated moving bed chromatography, enzymatic racemization, and a concentration system to produce pure enantiomers. Extract: undesired enantiomer solution; raffinate: desired enantiomer solution; fixed bed reactor containing an immobilized enzyme to racemize the undesired enantiomer. Concentration system: concentration of the extract solution. Both streams (racemic solution and eluent) are recycled and feed into the SMB system.

4.2. Supercritical fluid simulated moving bed

Supercritical fluid chromatography (SFC) is a powerful tool for the separation of compounds with very similar structure and volatility, as the case of enantiomers.[309] The use of a supercritical fluid as a mobile phase presents some advantages over liquid chromatography such as higher separation efficiency and reduced purification time (due to higher flow rates).[310] Consequently, it reduces solvent consumption and cost and increases productivity defined as racemate processed per unit mass of stationary phase and per unit time.[311] Moreover it is not necessary to concentrate the solute solution from the eluent.[310] The advantages and applications of supercritical fluid chromatography for enantioseparation are described in the following reviews.[311–320]

When merging simulated moving bed with supercritical fluid chromatography technologies it leads to a purification procedure with unique characteristics with advantages of both techniques, named Supercritical fluid simulated moving bed (SFC-SMB). In 1996, Clavier *et al.*[321] described for the first time the fusion between the two chromatography methods. The system consisted of a simulated moving bed unit containing SFC separation columns and supercritical CO_2 as eluent. Essentially, the elution strength of supercritical eluents varies with pressure and temperature gradients.[313] One year later, Mazzotti *et al.*[322] described an isocratic mode (pressure constant along the zones) and a pressure gradient mode (a gradient is imposed along the zones) for the development of optimal design and procedures to SFC-SMB units.

In 2001, Denet *et al.*[323] described the first enantioseparation in an SFC-SMB pilot unit with eight columns and four sec-

Open Access Article. Published on 20 May 2022. Downloaded on 14/09/2025 22:14:34.
This article is licensed under a Creative Commons Attribution-NonCommercial 3.0 Unported Licence.

Table 12 Overview of chiral resolution studies using SFC-SMB

Product	Chiral stationary phase	Eluent	Temp. (°C)	Pressure (bar)	Purity	Ref.
Tetralol enantiomers	Chiralcel OD	CO_2 modified with ethanol (5.4 wt%)	40	200/150	>97%	323
(*S*)-Ibuprofen	Kromasil CHI-TBB	CO_2 modified with isopropanol	40	171	>98%	310
Bi-naphthol	Kromasil CHI-DMB	CO_2 modified with isopropanol	40	160	—	325
1-Phenyl-1-propanol	Chiralcel OD	CO_2 modified with methanol (2.6 wt%)	30	180	>98%	326

tions. Complete resolution of two tetralol enantiomers was achieved in pressure-gradient mode at 200 bar at zones 1 and 2 and 150 bar at zones 3 and 4. Peper *et al.*[310] developed an SFC-SMB process with eight custom-made columns packed with Kromasil CHI-TBB for the resolution of a racemic mixture of ibuprofen (Table 12).

The authors tested 2/2/2/2 and the 2/2/3/1 columns configuration while column length, operating pressure, operating temperature, and content of modifier were kept constant. The feed concentration was also studied. Purities higher than 98% were obtained. In another publication, the co-workers[324] compared batch-SFC and SFC-SMB methods for racemic mixtures of tocopherol and ibuprofen from an economical point of view (*e.g.* product price, cost of process). Johannsen *et al.*[325] published the resolution development of bi-naphthol enantiomers. The influence of the modifier, modifier content, and column configuration on the productivity of the SFC-SMB process was investigated by simulation. The authors found that a six-column configuration (1/2/2/1) is adequate for the separation of bi-naphthol on Kromasil CHI-DMB.

In 2005, resolution of 1-phenyl-1-propanol by SFC-SMB was described by Rajendran *et al.*[326] in an eight Chiralcel-OD columns pilot unit. Complete separation was achieved at low feed concentrations. The solvent consumption was substantially lower than in SMB chromatographic systems.

In 2007, Kaemmerer *et al.*[327] determined that with an SFC-SMB, most of the carbon dioxide is recycled, and the solvent consumption is 76% lower. Since the desired compound is collected in a concentrated solution because the main part of the mobile phase is CO_2, the liquified gas is evaporated by decreasing the system pressure. Consequently, the time and the energy spent to evaporate the gas are lower than distilling the liquid eluent from liquid chromatographic systems.

In 2018, Johannsen and Brunner[309] used an SCF-SMB system to separate *cis*-/*trans*-phytol and α/δ-tocopherol isomers.

Sustainability considerations. The key advantage of an SMB process over batch chromatography is the cost-effective potential to enhance productivities and to reduce the solvent consumption compared to conventional discontinuous processes.[264,265]

Most chromatographic methods are not considered environmentally friendly and do not follow the principles of green chemistry. Improvements by eliminating hazardous reagents and reducing the use of flammable and toxic solvents must be put into practice.

Improvements should be done by replacing hazardous solvents with greener alternative ones (*e.g.*, acetonitrile and methanol by ethanol; ionic liquids).

The use of carbon dioxide in the form of a supercritical fluid offers a substitute for organic solvent. Also, it has low viscosity and high diffusivity that allows high flow rates and faster separations. Consequently, carbon dioxide promotes the reduction of organic solvent usage, elimination of waste, and reduction of treatment costs.[328]

5. Other resolution techniques

5.1. Continuous enzyme-mediated kinetic resolution

Kinetic resolution consists of the consumption of one of the two enantiomers in a chemical reaction. Through this difference, an excess of the less-reactive enantiomer is created, the concentration of which goes through a maximum before it disappears on full completion of the reaction.[11]

Enzymes began to be frequently used as catalysts on an industrial scale due to their enantioselectivity, substrate specificity, and ability to promote reactions under mild conditions.[329] To minimize the environmental impact of a chemical transformation, it has been explored the use of $scCO_2$ as the reaction solvent.

$ScCO_2$ has been identified as a green solvent with significant potential for industrial use as it provides a clean, non-toxic, non-flammable, and tunable solvent system that is easily removed.[330,331]

Continuous-flow kinetic resolution of racemic 1-phenylethanol (99.7 ee_S% and 47% yield) in $scCO_2$, was described by Matsuda *et al.*[332] with productivities 400 times higher than the batch procedure. The authors used an immobilized lipase (Novozym) to perform the kinetic resolution. Hobbs *et al.*[329] also carried out the resolution of 1-phenylethanol in $scCO_2$ system but using cross-linked enzyme aggregates (93 ee_S%). The interesting results showed that it is possible to expand the use of a continuous flow system by the incorporation of two reactors linked in series. The first reactor was used for the metal-catalyzed hydrogenation of acetophenone and the second reactor for immobilized lipase to catalyze the kinetic resolution of the resulting (*S*)-1-phenylethanol.

Water-immiscible ionic liquids (ILs) have recently emerged as exceptionally interesting green non-aqueous reaction media for bio-transformations (**P5**). Biphasic systems based on ILs and $scCO_2$ provide an integral green bioprocess in non-

Open Access Article. Published on 20 May 2022. Downloaded on 14/09/2025 22:14:34.
This article is licensed under a Creative Commons Attribution-NonCommercial 3.0 Unported Licence.

aqueous media, where both the resolution and extraction steps are coupled in efficient reaction/separation processes.[333]

Likewise, Reetz *et al.*[331] described the application of ILs as solvents and $scCO_2$ as extractants of the desired products for lipase-catalyzed kinetic resolution of chiral secondary alcohols. The co-workers demonstrated how the approach allows the combination of enzymatic catalytic esterification with highly efficient enantiomer separation in a continuous flow operation avoiding the use of organic solvents.

In 2009, Lozano *et al.*[333] also applied the IL-$scCO_2$ system to the continuous-flow kinetic resolution of racemic 1-phenylethanol using immobilized lipase (Novozym 435) and acidic zeolite catalysts having obtained enantioselectivities up to 97%.

Continuous-flow kinetic resolution of amines can be performed with immobilized transaminases as described by Molnár *et al.*[334] The authors immobilized the whole-cell (*E. coli* containing overexpressed transaminases) and filled it in packed columns. The racemic solution was fed into the packed bed and a minimum of 98 ee% was obtained.

Enzyme mediated kinetic resolution presents many advantages namely the high stereoselectivity, the possibility of operation in continuous mode, the inherent ease of scalability, and the energy-saving due to the used mild conditions. The main drawback of the enzyme-mediated kinetic resolution is that the activity decreases after a cycle period that must be determined.

The use of $scCO_2$ as solvent at least follows the first principle of green chemistry. It prevents waste (**P1**), it is an energy-efficient operation (**P6**), and do not use of organic solvents (**P12**) minimizing the risks of explosions and fires.[335]

5.2. Multistage enantioselective liquid–liquid extraction

Liquid–liquid extraction is a very known unit operation that might be operated in a continuous countercurrent mode to fractionate the racemate into its enantiomers, which is advantageous when scaling up.[336] Enantioselective liquid–liquid extraction (ELLE) is an attractive alternative for commercial operation but based on the available literature, it still needs development towards commercialization and improvement of efficiency.[337] Such as liquid membrane separation, ELLE is based on the selective recognition of one of the enantiomers by a chiral selector.[338]

Holbach *et al.* reported the continuous countercurrent flow experiments using a process intensified extraction column to separate a racemic mixture of phenylsuccinic acid in water and hydroxypropyl-β-cyclodextrin as the extractant in *n*-decanol.[338] Both enantiomers were separated with an enantiomeric excess of up to 60% and yields up to 80%. However, the high number of required extraction stages for a complete separation reveals the necessity of efficient equipment with many equilibrium stages.

Combining efficient mixing of two immiscible liquids with fast phase separation, the centrifugal contact separator (CCS) is a compact continuous flow device that seems perfectly fit for continuous operation. In addition, high centrifugal forces and preeminent mass-transfer characteristics of CCS make it suitable for use in process intensification of ELLE.[339]

Schuur *et al.*[337,340] reported the use of centrifugal contactor separator (CCS) equipment for continuous ELLE. In a CCS, two immiscible liquids are contacted and subsequently separated. These two-unit operations combined in one allows a more energy-efficient separation. The authors applied a countercurrent operated pilot-scale cascade of six CCS devices to a system composed of racemic 3,5-dinitrobenzoyl-(*R*,*S*)-leucine in water and a cinchona alkaloid as the extractant dissolved in 1,2-dichloroethane.

Continuous CCS seems highly suitable for ELLE, moreover, only a small amount of the host/extractant needs to be available to separate larger amounts of enantiomers in a continuous flow mode (60 g to separate 17.7 kg racemate). In a multistage countercurrent process approach is not necessary to achieve a complete separation of enantiomers in a single stage and therefore the selectivity requirements of the extractant/host are not so narrow.[336]

Tang *et al.* described the continuous ELLE of 4-nitro-D,L-phenylalanine in water using $PdCl_2${(*S*)-BINAP} as an extractant in 1,2-dichloroethane,[341] the continuous ELLE of amino-(4-nitro-phenyl)-acetic acid enantiomers in water using $CuPF_6${(*S*)-BINAP} in 1,2-dichloroethane[339] in a countercurrent cascade of 10 CCSs. The minimum number of stages for full separation of both racemic mixtures was calculated and a minimum value of 14 was obtained for >97% enantiomeric excess at both streams.

The co-workers also performed the continuous separation of α-cyclohexyl-mandelic acid[342] and phenylsuccinic acid[343] enantiomers using hydroxyphenyl-β-cyclodextrin as extractant dissolved in 1,2-dichloroethane.

Environmentally friendly and versatile extractants should be considered during development and host recycling should be performed to not generate any waste. Moreover, in 2007, alternatives to halogenated solvents were identified by the ACS Green Chemistry Institute Pharmaceutical Roundtable (ACS GCIPR) as a key subject in which more research was required.[344] The motivation for identifying alternatives to halogenated solvents is diverse and includes environmental health and safety concerns, economic and disposal costs, and regulatory and legal frameworks.[345]

5.3. Countercurrent chromatography

Countercurrent chromatography (CCC) is an effective separation technique based on the liquid–liquid partitioning of solutes in a solution of two non-miscible solvents.[346,347] Therefore, the mobile and stationary phases in the chromatographic process are liquids. The conventional column we are used to thinking in traditional liquid chromatography is substituted by an instrument that produces a centrifugal field used to maintain stationary one of the liquid phases called a centrifugal partition chromatograph.[346] Another technique would be high-speed CCC where it is used a specific apparatus. An advantage of CCC is that the superficial area of the liquid

Open Access Article. Published on 20 May 2022. Downloaded on 14/09/2025 22:14:34.
This article is licensed under a Creative Commons Attribution-NonCommercial 3.0 Unported Licence.

stationary phase is much higher than the one found in chromatography with solid support.[348]

Regarding the separation of enantiomers, the application of CCC can be of great interest since this technique offers the possibility to produce enantiomerically pure compounds at a lower cost compared to conventional liquid chromatography and had the advantages of high load capacity, low solvent consumption, and easy scaling-up to preparative scale.[349,350]

As for other enantioselective separation techniques, in CCC a chiral host is needed to establish an enantioselective environment and it is chosen based on the solubility properties in the stationary phase. The racemic mixture is partitioned between the two phases of the biphasic solvent system.[346]

Commonly, the two-phase solvent systems used in CCC for enantioseparation are constituted by an organic solvent, and a strongly polar solution, often aqueous. The *enantio*-recognition occurs in the stationary phase, either organic or aqueous, where the chiral selector is retained. Exhaustive reviews on the enantiomeric separations in CCC were published by Foucault[348] and Huang *et al.*[351]

The attention of some related researchers was concentrated on looking for ways of improving the separation efficiency of chiral separation by CCC. Novel methods such as multiple dual mode elution[352] that consist of switching alternatively between reversed and normal phase operation during the experiment was applied for the resolution of (*S*)-naproxen derivative.[353] The recycling elution mode (or closed-loop recycling elution mode) consists in recycling the effluent that leaves the chromatograph was applied for the separation of amlodipine besilate,[354] oxybutynin,[355] and naproxen[356] enantiomers. This last methodology has the greener advantage that would not consume extra solvent because the mobile phase is recycled in a closed-loop. These methods partly mitigate the resolution limitation of CCC in enantioseparation, but more studies must be performed in the future.

As far as we know, no continuous countercurrent chromatography protocol was described for enantiomeric separation, all described examples were performed in discontinuous mode. Therefore, the envisagement of a semi-continuous or continuous CCC technology would improve the capacity and the productivity of the technique.[346] A new system was patented by Couillard *et al.*,[357] which describes a continuous centrifugal partition chromatography process that might apply to the separation of enantiomers.[346] This system is characterized by the injection of the feed solution at an intermediate point of the centrifugal chromatograph followed by sequential feeding of a dense solvent phase and a light solvent phase from opposite ends of the column.

Likewise, intermittent counter-current extraction was described by Sutherland *et al.*[358] consisting of a quasi-continuous counter-current chromatography process used to separate caffeine, vanillin, naringenin, and carvone and might be used for enantiomeric separation.

6. General conclusion and outlook

Over the last decades, the continuous mode has gained the interest of industry and academia due to its many advantages over discontinuous procedures including better reproducibility, yields,[49,51–53] shorter development period, smaller equipment footprint, and precise control of process parameters. Even with these advantages, the continuous chiral resolution is not frequently used as often as it should be. This review was aimed to introduce the different continuous approaches – and highlight some case studies – Fig. 20.

A preferential crystallization process is only feasible for conglomerate-forming systems, by seeding of a racemic or enantiomerically enriched solution with crystals of the preferred pure enantiomer, control over the crystallizing enantiomer is obtained. It is a cost-effective method to obtain crystals of a single enantiomer. Unfortunately, only 10% of the racemic mixtures belong to the conglomerate forming group, consequently, the scope of this technique is limited.

It was discussed different possible setups that can be explored during process development. There is no better setup, all should be considered depending on the project, availability of equipment, and level of expertise. In general, two-coupled crystallizers and a feed tank offer more possibilities since they can continuously feed racemic solution and, in separate vessels, isolate individual crystalline enantiomers. It also offers the possibility to recover from a failed resolution simply by heating the crystallizers to a temperature that would dissolve all the formed crystals (**P1**). Also, the isolated undersired enantiomer might be racemized and submitted to a new preferential crystallization procedure to obtain higher yields processes (**P1**). This possibility may be the best advantage of continuous preferential crystallization. In summary, continuous preferential crystallization offers higher productivities and improved process control.

If the racemic mixture does not belong to the conglomerate forming group, continuous crystallization (following the classical approach where a diastereomer is previously prepared) can be done although it does not follow **P1**, **P2** and **P8**.

By developing a continuous crystallization procedure, more control on the morphology and particle size distribution is obtained, the development can be faster, and the reproducibility can be enhanced.

The membrane-based enantiomeric resolution has attracted attention due to its inherent advantages namely ease of scale-up, low footprint, energy consumption, and continuous mode of operation (**P6**). Membranes can be separated into two main groups: liquid membranes and solid membranes. The liquid membranes have been extensively investigated for the separation of enantiomers due to their high separation factor and increased mass transfer. Hollow fiber membrane modules present high surface area per volume resulting in a relatively compact system, consequently very easy for scaling-up. The literature demonstrates how the solute exchange between two crystallizers separated by a hollow-fiber membrane module results in both high purity and high yield enantiomeric separ-

Open Access Article. Published on 20 May 2022. Downloaded on 14/09/2025 22:14:34.
This article is licensed under a Creative Commons Attribution-NonCommercial 3.0 Unported Licence.

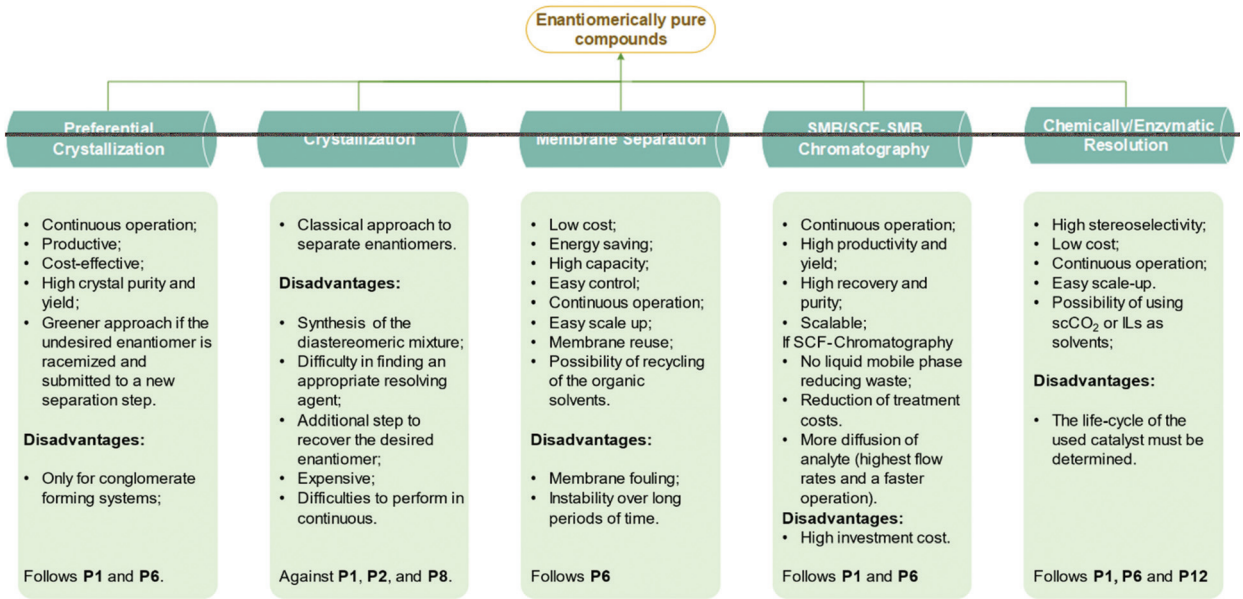

Fig. 20 Semi-continuous and continuous approaches to obtain enantiomerically pure compounds.

ation process. This option combines the high selectivity and mass transfer of liquid membranes with the stability and mechanical strength of solid membranes. The results gathered in this review show how efficient supported liquid membranes can be for enantiomeric resolution. Moreover, there are HF modules available in the market which turns this option easier for industrial application and continuous or semi-continuous operation. Solid membranes with inherent chiral polymers and polymeric membranes functionalized with a chiral selector are the most classical type. In recent years, composite, graphene oxide, and MOFs membranes have been studied to find an optimal combination of membrane stereo-selectivity, permeability, and mechanical stability. The results show that they are a promising type of membrane material but more studies on the preparation, stereo-selectivity, waste management, membrane recycling, and use on a large scale must be carried on. Molecularly imprinted membranes are a promising field in which a polymer network is prepared with specific recognition sites for a target template molecule. However, it would be valuable to see this technology being applied at a higher scale and in a cGMP setting for enantiomeric resolution.

Looking out at all the studies described herein, it seems that complete enantioseparation of a racemic mixture through one cycle process with membranes is not feasible. Multi-cycle operation processes may be the path forward to achieve better separation, even though the number of cycles required to achieve it will likely affect the productivity of the operation. The combination of two technologies as continuous crystallization and membrane separation, as described by Svang-Ariyaskul,[126] might be a good setup to achieve an efficient and greener semi-continuous enantiomeric separation.

The combination of the simulated moving bed technique with supercritical fluid chromatography leads to a separation unit with great advantages. Namely, the increase of mass transfer due to the higher diffusivities of solutes in supercritical fluids increases the separation efficiency and decreases pressure drop (**P1**). Faster cycles (by using higher flow rates), and a reduction of organic solvents (2–10 times lower)[313] do not only contribute to a greener, environmentally friendly separation process but also reduce the costs in theory.[311,324] We may consider the fact that an SFC system requires additional heating and cooling not required for HPLC systems, and thus, additional energy requirements. At the inlet of the unit, the feed containing carbon dioxide must be cooled to a liquid, at the outlet during depressurization it is necessary to heat. Finally, to recycle carbon dioxide is required additional cooling to condense the resulting gas. In total, an operating SFC unit is heated and cooled simultaneously at several locations.[312] Despite the advantages here mentioned to operating an SMB unit under supercritical conditions, not many studies about enantiomer resolution in pilot scales have been reported in the literature. This may be due to the high cost of assembling an SMB pilot unit under supercritical conditions.

There is no better approach for enantiomeric separation, it depends on each case. But we firmly believe that with this review paper, the readers might have an overall idea of each possible technique, when to use each technique, and which green chemistry principles it follows.

More studies must be performed to improve the greenness of enantiomeric separation since it is still not a green operation. The mindset of chemists and engineers is changing, and the environmental impact of the developed processes is a real preoccupation. Therefore, there is a trend on developing processes as much greener as it can be. With this review paper it is possible to identify what has already been achieved and what should be kept in mind when developing new processes to improve the greener impact on enantiomeric separation.

 This journal is © The Royal Society of Chemistry 2022

Open Access Article. Published on 20 May 2022. Downloaded on 14/09/2025 22:14:34.
This article is licensed under a Creative Commons Attribution-NonCommercial 3.0 Unported Licence.

Abbreviations

API	Active pharmaceutical ingredient
(D)-DTTA	Di-*p*-toluyl-(D)-tartaric acid
ACN	Acetonitrile
AcOH	Acetic acid
ATR	Attenuated total reflectance
BINAP	2,2′-Bis(diphenylphosphino)-1,1′-binaphthyl
BLM	Bulk liquid membrane
CCC	Countercurrent chromatography
CD	Cyclodextrin
CNT	Carbon nanotubes
COFs	Covalent organic frameworks
CPC	Coupled preferential crystallizer
CPP	Critical process parameters
CQAs	Critical quality attributes
D2EHPA	Di(2-ethylhexyl)phosphoric acid
DACH	(*S*,*S*)-1,2-Diaminocyclohexane
DBTA	*O*,*O*-Dibenzoy(L)-(2*S*,3*S*)-tartaric acid
DFT	Density functional theory
DMAC	Dimethylacetamide
DMSO	Dimethylsulfoxide
E_a	Activation energy
ee	Enantiomeric excess
EGDMA	Ethylene glycol dimethacrylate
ELM	Emulsion liquid membrane
EtOH	Etanol
FBC	Fluidized bed crystallizer
FDA	Food and Drugs Administration
Glu	Glutamic acid
GO	Graphene oxide
HF	Hollow fiber
HOFs	Hydrogen-bonded organic frameworks
ILs	Ionic liquids
IPA	Isopropanol
MAA	Methacrylic acid
MeOH	Metanol
MIM	Molecularly imprinted membranes
MMM	Mixed matrix membranes
MOFs	Metal–organic frameworks
MPD	*m*-Phenylene diamine
MSMPR	Mixed-suspension mixed-product-removal
MWCO	Molecular weight cut-off
NMP	*N*-Methylpyrrolidone
PAT	Process Analytical Technologies
PC	Preferential crystallization
PFC	Plug flow crystallizers
Phe	Phenylalanine
PLGA	Poly-(L)-glutamic acid
poly-PSPA	Poly-[dimethyl(10-pinanyl)silyl]phenylacetylene
PVDF	Polyvinylidene fluoride
$ScCO_2$	Supercritical carbon dioxide
SFC	Supercritical fluid chromatography
SLM	Supported liquid membrane
SMB	Simulated moving bed
TFA	Trifluoroacetic acid
TMC	1,3,5-Trimesoyl chloride
Trp	Tryptophan
Tyr	Tyrosine
α	Separation factor

Conflicts of interest

There are no conflicts to declare.

Acknowledgements

The authors thank Hovione Farmaciência S.A. for funding this project. C. A. M. A acknowledge Fundação para a Ciência e Tecnologia (FCT) for financial support (PTDC/QUIQOR/32008/2017, PTDC/QUI-QOR/1131/2020, UIDB/04138/2020 and UIDP/04138/2020). The project leading to this application has received funding from the European Union's Horizon 2020 research and innovation programme under grant agreement No. 951996.

Notes and references

1 M. L. Pasteur, *C. R. Seances Acad. Sci.*, 1848, **26**, 535–539.
2 Food and Drugs Administration (FDA), Development of New Stereoisomeric Drugs, https://www.fda.gov/regulatory-information/search-fda-guidance-documents/development-new-stereoisomeric-drugs, (accessed 24 January 2021).
3 Eur. Med. Agency, *Investigation of Chiral Active Substances Guideline*, 1994, pp. 381–391.
4 B. L. He and D. K. Lloyd, *Chiral methods*, Elsevier Ltd, 2020.
5 Nextmsc, Chiral Chemicals Market by Technology (Traditional Separation Method), Asymmetric Preparation Method (Asymmetric Synthesis Method and Asymmetric Catalysis Method), Biological Separation Method, and Other Separation Methods, by Application (Pharmaceuticals, https://www.nextmsc.com/report/chiral-chemicals-market, (accessed 29 January 2021).
6 FactMR, Chiral Chemicals Market's Reliance on Demand from Pharmaceutical Industry Continues Unabated: Fact.MR's Study, https://www.accesswire.com/623438/Chiral-Chemicals-Markets-Reliance-on-Demand-from-Pharmaceutical-Industry-Continues-Unabated-FactMRs-Study, (accessed 29 January 2021).
7 S. W. Smith, *Toxicol. Sci.*, 2009, **110**, 4–30.
8 J. M. Daniels, E. R. Nestmann and A. Kerr, *Ther. Innov. Regul. Sci.*, 1997, **31**, 639–646.
9 S. K. Branch and A. J. Hutt, in *Drug Stereochemistry - Analytical Methods and Pharmacology*, CRC Press, 3rd edn, 2012, pp. 240–273.
10 N. R. Srinivas, R. H. Barbhaiya and K. K. Midha, *J. Pharm. Sci.*, 2001, **90**, 1205–1215.

Open Access Article. Published on 20 May 2022. Downloaded on 14/09/2025 22:14:34.
This article is licensed under a Creative Commons Attribution-NonCommercial 3.0 Unported Licence.

11 H. Lorenz and A. Seidel-Morgenstern, *Angew. Chem., Int. Ed.*, 2014, **53**, 1218–1250.
12 L. A. Nguyen, H. He and C. Pham-huy, *Int. J. Biomed. Sci.*, 2006, **2**, 85–100.
13 J. Tomaszewski and M. M. Rumore, *Drug Dev. Ind. Pharm.*, 1994, **20**, 119–139.
14 X. Yuan, L. Wang, G. Liu, G. Dai and K. Tang, *Chirality*, 2019, **31**, 445–456.
15 C. Rougeot and J. E. Hein, *Org. Process Res. Dev.*, 2015, **19**, 1809–1819.
16 T. Vetter, C. L. Burcham and M. F. Doherty, *AIChE J.*, 2015, **61**, 2810–2823.
17 W. Bi, M. Tian and K. H. Row, *Analyst*, 2011, **136**, 379–387.
18 M. Kaspereit, S. Swernath and A. Kienle, *Org. Process Res. Dev.*, 2012, **16**, 353–363.
19 P. Anastas and N. Eghbali, *Chem. Soc. Rev.*, 2010, **39**, 301–312.
20 L. Rogers and K. F. Jensen, *Green Chem.*, 2019, **21**, 3481–3498.
21 S. G. Newman and K. F. Jensen, *Green Chem.*, 2013, **15**, 1456–1472.
22 J. Orehek, D. Teslić and B. Likozar, *Org. Process Res. Dev.*, 2021, **25**, 16–42.
23 J. Chen, B. Sarma, J. M. B. Evans and A. S. Myerson, *Cryst. Growth Des.*, 2011, 887–895.
24 G. Coquerel, *Chem. Soc. Rev.*, 2014, **43**, 2286–2300.
25 T. Vetter, C. L. Burcham and M. F. Doherty, *Chem. Eng. Sci.*, 2014, **106**, 167–180.
26 M. L. Pasteur, *C. R. Seances Acad. Sci.*, 1853, **37**, 162–166.
27 G. Levilain and G. Coquerel, *CrystEngComm*, 2010, **12**, 1983–1992.
28 K. S. Kim, WO1998/13344, 1998.
29 P. G. Holton, US4515811, 1980.
30 A. S. Dunn, V. Svoboda, J. Sefcik and J. H. Ter Horst, *Org. Process Res. Dev.*, 2019, **23**, 2031–2041.
31 N. Sato, T. Uzuki, K. Toi and T. Akashi, *Agric. Biol. Chem.*, 1969, **33**, 1107–1108.
32 C. Viedma, *Phys. Rev. Lett.*, 2005, **94**, 1–4.
33 M. Iggland and M. Mazzotti, *Cryst. Growth Des.*, 2011, **11**, 4611–4622.
34 C. Viedma, J. E. Ortiz, T. de Torres, T. Izumi and D. G. Blackmond, *J. Am. Chem. Soc.*, 2008, **130**, 15274–15275.
35 W. L. Noorduin, T. Izumi, A. Millemaggi, M. Leeman, H. Meekes, W. J. P. Van Enckevort, R. M. Kellogg, B. Kaptein, E. Vlieg and D. G. Blackmond, *J. Am. Chem. Soc.*, 2008, **130**, 1158–1159.
36 I. Baglai, M. Leeman, M. Kellogg and W. L. Noorduin, *Org. Biomol. Chem.*, 2019, **17**, 35–38.
37 L. C. Sogutoglu, R. R. E. Steendam, H. Meekes, E. Vlieg and F. P. J. T. Rutjes, *Chem. Soc. Rev.*, 2015, **44**, 6723–6732.
38 H. Lorenz, A. Perlberg, D. Sapoundjiev, M. P. Elsner and A. Seidel-Morgenstern, *Chem. Eng. Process.*, 2006, **45**, 863–873.
39 S. Srisanga and J. H. Ter Horst, *Cryst. Growth Des.*, 2010, **10**, 1808–1812.
40 K. Petruševska-Seebach, A. Seidel-Morgenstern and M. P. Elsner, *Cryst. Growth Des.*, 2011, **11**, 2149–2163.
41 G. Coquerel, M. N. Petit and R. Bouaziz, US6022409, 2000.
42 E. Ndzié, P. Cadinael, A. Schoofs and G. Coquerel, *Tetrahedron: Asymmetry*, 1997, **8**, 2913–2920.
43 G. Coquerel, G. Tauvel and M. N. Petit, US8034948B2, 2011.
44 L. Courvoisier, E. Ndzié, M. Petit, U. Hedtmann, U. Sprengard and G. Coquerel, *Chem. Lett.*, 2001, **30**, 364–365.
45 F. X. Gendron, J. Mahieux, M. Sanselme and G. Coquerel, *Cryst. Growth Des.*, 2019, **19**, 4793–4801.
46 F. Czapla, H. Haida, M. P. Elsner, H. Lorenz and A. Seidel-Morgenstern, *Chem. Eng. Sci.*, 2009, **64**, 753–763.
47 C. Gervais, P. Cardinae and S. Petit, *J. Phys. Chem. B*, 2002, **106**, 646–652.
48 S. Bellies, P. Cardinael, E. Ndzié, S. Petit and G. Coquerel, *Chem. Eng. Sci.*, 2001, **56**, 2281–2294.
49 J. Li, T. C. Lai, B. L. Trout and A. S. Myerson, *Cryst. Growth Des.*, 2017, **17**, 1000–1007.
50 Y. Ma, S. Wu, E. Genito, J. Macaringue, T. Zhang, J. Gong and J. Wang, *Org. Process Res. Dev.*, 2020, **24**, 1785–1801.
51 K. Galan, M. J. Eicke, M. P. Elsner, H. Lorenz and A. Seidel-morgenstern, *Cryst. Growth Des.*, 2015, **15**, 1808–1818.
52 E. Temmel, J. Gänsch, A. Seidel-morgenstern and H. Lorenz, *Crystals*, 2020, **10**, 394.
53 J. H. Chaaban, K. Dam-Johansen, T. Skovby and S. Kiil, *Org. Process Res. Dev.*, 2013, **17**, 1010–1020.
54 F. Cameli, C. Xiouras and G. D. Stefanidis, *CrystEngComm*, 2020, **22**, 3519–3525.
55 R. Lakerveld, B. Benyahia, R. D. Braatz and P. I. Barton, *AIChE J.*, 2013, **59**, 3671–3685.
56 S. Mascia, P. L. Heider, H. Zhang, R. Lakerveld, B. Benyahia, P. I. Barton, R. D. Braatz, C. L. Cooney, J. M. B. Evans, T. F. Jamison, K. F. Jensen, A. S. Myerson and B. L. Trout, *Angew. Chem., Int. Ed.*, 2013, **52**, 12359–12363.
57 S. Ferguson, G. Morris, H. Hao, M. Barrett and B. Glennon, *Chem. Eng. Sci.*, 2012, **77**, 105–111.
58 J. L. Quon, H. Zhang, A. Alvarez, J. Evans, A. S. Myerson and B. L. Trout, *Cryst. Growth Des.*, 2012, **12**, 3036–3044.
59 A. J. Alvarez and A. S. Myerson, *Cryst. Growth Des.*, 2010, **10**, 2219–2228.
60 D. Zhang, S. Xu, S. Du, J. Wang and J. Gong, *Engineering*, 2017, **3**, 354–364.
61 C. Darmali, S. Mansouri, N. Yazdanpanah and M. W. Woo, *Ind. Eng. Chem. Res.*, 2019, **58**, 1463–1479.
62 B. Wood, K. P. Girard, C. S. Polster and D. M. Croker, *Org. Process Res. Dev.*, 2019, **23**, 122–144.
63 M. P. Elsner, D. F. Menéndez, E. A. Muslera and A. Seidel-Morgenstern, *Chirality*, 2005, **17**, 183–195.
64 A. A. Rodrigo, H. Lorenz and A. Seidel-morgenstern, *Chirality*, 2004, **16**, 499–508.
65 S. Qamar, K. Galan, M. Peter, I. Hussain and A. Seidel-morgenstern, *Chem. Eng. Sci.*, 2013, **98**, 25–39.
66 A. Majumder and Z. K. Nagy, *Pharmaceutics*, 2017, **9**, 1–19.

 This journal is © The Royal Society of Chemistry 2022

Open Access Article. Published on 20 May 2022. Downloaded on 14/09/2025 22:14:34.
This article is licensed under a Creative Commons Attribution-NonCommercial 3.0 Unported Licence.

67 S. Y. Wong, A. P. Tatusko, B. L. Trout and A. S. Myerson, *Cryst. Growth Des.*, 2012, **12**, 5701–5707.
68 I. Radoljub, J. J. De Yoreo and D. Robert, *Cryst. Growth Des.*, 2004, **4**, 1045–1052.
69 D. Zhang, S. Xu, S. Du, J. Wang and J. Gong, *Engineering*, 2017, **3**, 354–364.
70 M. Jiang and R. D. Braatz, *CrystEngComm*, 2019, **21**, 3534–3551.
71 M. Midler, US3510266, 1970.
72 M. Midler, US3892539, 1975.
73 E. J. J. Grabowski, *Chirality*, 2005, **17**, 249–259.
74 D. Binev and H. Lorenz, *Chem. Eng. Sci.*, 2015, **133**, 116–124.
75 T. Kollges and T. Vetter, *Cryst. Growth Des.*, 2018, **18**, 1686–1696.
76 K. Ito, T. Akashi, S. Tatsumi, Midarebashi, K. Shi and K. Ken, US3260744, 1966.
77 M. Eicke, A. Seidel-Morgenstern and M. P. Elsner, *Chem. Eng. Trans.*, 2009, **17**, 651–656.
78 S. Qamar, M. Peter Elsner, I. Hussain and A. Seidel-Morgenstern, *Chem. Eng. Sci.*, 2012, **71**, 5–17.
79 J. H. Chaaban, K. Dam-johansen, T. Skovby and S. Kiil, *Org. Process Res. Dev.*, 2014, **18**, 601–612.
80 T. Köllges and T. Vetter, *Cryst. Growth Des.*, 2017, **17**, 233–247.
81 M. Mangold, D. Khlopov, E. Temmel, H. Lorenz and A. Seidel-Morgenstern, *Chem. Eng. Sci.*, 2017, **160**, 281–290.
82 M. Mangold, N. Huskova, J. Gänsch and A. Seidel-morgenstern, *Processes*, 2020, **8**, 1–16.
83 M. P. Elsner, G. Ziomek and A. Seidel-Morgenstern, *Chem. Eng. Sci.*, 2007, **62**, 4760–4769.
84 M. P. Elsner, G. Ziomek and A. Seidel-Morgenstern, *Chem. Eng. Sci.*, 2011, **66**, 1269–1284.
85 M. P. Elsner, G. Ziomek and A. Seidel-Morgenstern, *AIChE J.*, 2009, **55**, 640–649.
86 S. Qamar, K. Galan and A. Seidel-morgenstern, *Chem. Eng. Trans.*, 2013, **32**, 2053–2058.
87 G. Levilain, M. J. Eicke and A. Seidel-Morgenstern, *Cryst. Growth Des.*, 2012, **12**, 5396–5401.
88 M. J. Eicke, G. Levilain and A. Seidel-Morgenstern, *Cryst. Growth Des.*, 2013, **13**, 1638–1648.
89 E. Temmel, M. J. Eicke, F. Cascella, A. Seidel-morgenstern and H. Lorenz, *Cryst. Growth Des.*, 2019, **19**, 3148–3157.
90 D. Binev and H. Lorenz, *Cryst. Growth Des.*, 2016, **16**, 1409–1419.
91 A. Majumder, *Processes*, 2018, **6**, 1–17.
92 J. E. Hein, B. H. Cao, M. W. Meijden, M. Leeman and R. M. Kellogg, *Org. Process Res. Dev.*, 2013, **17**, 946–950.
93 J. E. Hein, B. Huynh Cao, C. Viedma, R. M. Kellogg and D. G. Blackmond, *J. Am. Chem. Soc.*, 2012, **134**, 12629–12636.
94 H. D. Baumgard, B. Haedke, J. Himmelreich and H. Judat, US6315966B1, 2001.
95 R. Xie, L. Y. Chu and J. G. Deng, *Chem. Soc. Rev.*, 2008, **37**, 1243–1263.
96 J. T. F. Keurentjes, L. J. W. M. Nabuurs and E. A. Vegter, *J. Membr. Sci.*, 1996, **113**, 351–360.
97 C. Fernandes, M. E. Tiritan and M. M. M. Pinto, *Symmetry*, 2017, **9**, 1–19.
98 M. Ulbricht, *J. Chromatogr. B: Anal. Technol. Biomed. Life Sci.*, 2004, **804**, 113–125.
99 E. van der Ent, *J. Membr. Sci.*, 2001, **185**, 207–221.
100 M. Yoshikawa and A. Higuchi, in *Encyclopedia of Membrane Science and Technology*, John Wiley & Sons, Inc., 2013.
101 Y. Lu, J. Y. Chan, H. Zhang, X. Li, Y. Nolvachai, P. J. Marriott, X. Zhang, G. P. Simon, M. M. Banaszak Holl and H. Wang, *J. Membr. Sci.*, 2021, **620**, 1–9.
102 J. J. Keating, S. Bhattacharya and G. Belfort, *J. Membr. Sci.*, 2018, **555**, 30–37.
103 S. Peacock, D. Walba, F. C. A. Gaeta, R. C. Helgeson and D. J. Cram, *J. Am. Chem. Soc.*, 1980, **102**, 2043–2052.
104 D. J. Cram and J. M. Cram, *Science*, 1974, **183**, 803–809.
105 M. Newcomb, J. L. Toner, R. C. Helgeson and D. J. Cram, *J. Am. Chem. Soc.*, 1979, **101**, 4941–4947.
106 T. J. Ward and K. D. Ward, *Anal. Chem.*, 2012, **84**, 626–635.
107 W. H. Pirkle and E. M. Doherty, US5080795, 1992.
108 A. Gössi, W. Riedl and B. Schuur, *J. Chem. Technol. Biotechnol.*, 2018, **93**, 629–644.
109 J. Ramkumar and S. Chandramouleeswaran, *Indian J. Adv. Chem. Sci.*, 2015, **3**, 293–298.
110 B. J. V. Verkuijl, A. J. Minnaard, J. G. De Vries and B. L. Feringa, *J. Org. Chem.*, 2009, **74**, 6526–6533.
111 H. M. Krieg, J. Lotter, K. Keizer and J. C. Breytenbach, *J. Membr. Sci.*, 2000, **167**, 33–45.
112 P. J. Pickering and J. B. Chaudhuri, *Chirality*, 1997, **9**, 261–267.
113 P. Dzygiel and P. Wieczorek, *J. Membr. Sci.*, 2000, **172**, 223–232.
114 E. V. Yurtov and M. Y. Koroleva, *Pet. Chem.*, 2014, **54**, 581–594.
115 P. J. Pickering and J. B. Chaudhuri, *J. Membr. Sci.*, 1997, **127**, 115–130.
116 D. Huang, Y. Long, W. Liu, Y. Hong, M. Zhong and S. Xu, in *Proceedings of the 5th International Conference on Information Engineering for Mechanics and Materials*, 2015, pp. 533–538.
117 D. Kong, Z. Zhou, H. Zhu, Y. Mao, Z. Guo, W. Zhang and Z. Ren, *J. Membr. Sci.*, 2016, **499**, 343–351.
118 Y. Zhao, X. Zhu, W. Jiang, H. Liu and B. Sun, *Molecules*, 2021, **26**, 1–30.
119 P. Dzygiel, P. Wieczorek, J. Å. Jonsson, M. Milewska and P. Kafarski, *Tetrahedron*, 1999, **55**, 9923–9932.
120 J. D. Clark, B. Han, A. S. Bhown and S. R. Wickramasinghe, *Sep. Purif. Technol.*, 2005, **42**, 201–211.
121 P. Dzygiel, P. Wieczorek and P. Kafarski, *J. Sep. Sci.*, 2003, **26**, 1050–1056.
122 E. Miyako, T. Maruyama, N. Kamiya and M. Goto, *Chem. Commun.*, 2003, **3**, 2926–2927.

Open Access Article. Published on 20 May 2022. Downloaded on 14/09/2025 22:14:34.
This article is licensed under a Creative Commons Attribution-NonCommercial 3.0 Unported Licence.

123 R. M. C. Viegas, C. A. M. Afonso, J. G. Crespo and I. M. Coelhoso, *J. Membr. Sci.*, 2007, **305**, 203–214.
124 F. Jiao, W. Yang, D. Huang, J. Yu, X. Jiang, F. Jiao, W. Yang, D. Huang and J. Yu, DOI: 10.1080/01496395.2012.659784.
125 C. A. M. Afonso and J. G. Crespo, *Angew. Chem., Int. Ed.*, 2004, **43**, 5293–5295.
126 A. Svang-Ariyaskul, W. J. Koros and R. W. Rousseau, *Chem. Eng. Sci.*, 2012, **77**, 35–41.
127 L. Zeng, Q. Liu, Q. Yi, K. Tang and B. Van Der Bruggen, *Ind. Eng. Chem. Res.*, 2020, **59**, 13735–13743.
128 A. Maximini, H. Chmiel, H. Holdik and N. W. Maier, *J. Membr. Sci.*, 2006, **276**, 221–231.
129 H. B. Ding, P. W. Carr and E. L. Cussler, *AIChE J.*, 1992, **38**, 1493–1498.
130 T. Takeuchi, R. Horikawa and T. Tanimura, *Anal. Chem.*, 1984, **56**, 1152–1155.
131 P. Hadik, L. P. Szabó and E. Nagy, *Desalination*, 2002, **148**, 193–198.
132 P. Hadik, L. Kotsis, M. Eniszné-Bódogh, L. P. Szabó and E. Nagy, *Sep. Purif. Technol.*, 2005, **41**, 299–304.
133 Z. Wang, C. Cai, Y. Lin, Y. Bian, H. Guo and X. Chen, *Sep. Purif. Technol.*, 2011, **79**, 63–71.
134 T. Prapasawat, A. W. Lothongkum and U. Pancharoen, *Chem. Pap.*, 2014, **68**, 180–189.
135 A. Svang-Ariyaskul, Dissertation Thesis, Georgia Institute of Technology, 2010.
136 A. Svang-Ariyaskul, W. J. Koros and R. W. Rousseau, *Chem. Eng. Sci.*, 2009, **64**, 1980–1984.
137 J. L. Lopez and S. L. Matson, *J. Membr. Sci.*, 1997, **125**, 189–211.
138 T. Börner, G. Rehn, C. Grey and P. Adlercreutz, *Org. Process Res. Dev.*, 2015, **19**, 793–799.
139 N. Sunsandee, N. Leepipatpiboon, P. Ramakul and U. Pancharoen, *Chem. Eng. J.*, 2012, **180**, 299–308.
140 N. Sunsandee, N. Leepipatpiboon and P. Ramakul, *Korean J. Chem. Eng.*, 2013, **30**, 1312–1320.
141 S. Lai, S. Tang, J. Xie, C. Cai, X. Chen and C. Chen, *J. Chromatogr. A*, 2017, **1490**, 63–73.
142 T. Aoki, S. Tomizawa and E. Oikawa, *J. Membr. Sci.*, 1995, **99**, 117–125.
143 C. Thoelen, M. De, E. Theunissen, Y. Kondo, I. F. J. Vankelecom, P. Grobet, M. Yoshikawa and P. A. Jacobs, *J. Membr. Sci.*, 2001, **186**, 153–163.
144 K. Taki, I. Arita, M. Satoh and J. Komiyama, *J. Polym. Sci., Part B: Polym. Phys.*, 1999, **37**, 1035–1041.
145 J. H. Kim, J. Jegal, J. H. Kim, K. Lee and Y. Lee, *J. Appl. Polym. Sci.*, 2003, **89**, 3046–3051.
146 J. H. Kim, J. H. Kim, J. Jegal and K. Lee, *J. Membr. Sci.*, 2003, **213**, 273–283.
147 S. Xie, W. Wang, P. Ai, M. Yang and L. Yuan, *J. Membr. Sci.*, 2008, **321**, 293–298.
148 A. Higuchi, M. Tamai, Y. A. Ko, Y. I. Tagawa, Y. H. Wu, B. D. Freeman, J. T. Bing, Y. Chang and Q. D. Ling, *Polym. Rev.*, 2010, **50**, 113–143.
149 T. Aoki, T. Fukuda, T. Kaneko, M. Teraguchi and M. Yagi, *J. Polym. Sci., Part A: Polym. Chem.*, 2004, **42**, 4502–4517.
150 S. Hazarika, *J. Membr. Sci.*, 2008, **310**, 174–183.
151 C. Ma, X. Xu, P. Ai, S. Xie, Y. Lv, H. Shan and L. Yuan, *Chirality*, 2011, **23**, 379–382.
152 L. M. Yuan, W. Ma, M. Xu, H. L. Zhao, Y. Y. Li, R. L. Wang, A. H. Duan, P. Ai and X. X. Chen, *Chirality*, 2017, **29**, 315–324.
153 X. Weng, J. E. Baez, M. Khiterer, M. Y. Hoe, Z. Bao and K. J. Shea, *Angew. Chem., Int. Ed.*, 2015, **54**, 11214–11218.
154 R. J. Petersen, *J. Membr. Sci.*, 1993, **83**, 81–150.
155 P. G. Ingole, K. Singh and H. C. Bajaj, *Desalination*, 2011, **281**, 413–421.
156 P. G. Ingole, H. C. Bajaj, D. N. Srivastava, B. Rebary and K. Singh, *Sep. Sci. Technol.*, 2013, **48**, 1777–1787.
157 P. G. Ingole, H. C. Bajaj and K. Singh, *Desalination*, 2014, **343**, 75–81.
158 K. Singh, S. Devi, H. C. Bajaj, P. Ingole, J. Choudhari and H. Bhrambhatt, *Sep. Sci. Technol.*, 2014, **49**, 2630–2641.
159 L. Miao, Y. Yang, Y. Tu, S. Lin, J. Hu, Z. Du, M. Zhang and Y. Li, *React. Funct. Polym.*, 2017, **115**, 87–94.
160 J. Gaálová, F. Yalcinkaya, P. Cuřínová, M. Kohout, B. Yalcinkaya, M. Koštejn, J. Jirsák, I. Stibor, J. E. Bara, B. Van der Bruggen and P. Izák, *J. Membr. Sci.*, 2020, **596**, 1–9.
161 Z. Zhou, D. Li, Q. Wu, T. Zheng, H. Yuan and N. Peng, *Chem. Eng. Res. Des.*, 2020, **160**, 437–446.
162 M. Gogoi, R. Goswami, P. G. Ingole and S. Hazarika, *Sep. Purif. Technol.*, 2020, **233**, 116061.
163 J. Ke, Y. Zhang, X. Zhang, Y. Liu, Y. Ji and J. Chen, *J. Membr. Sci.*, 2020, **597**, 117635.
164 G. Liu, J. Wanqin and X. Nanping, *Chem. Soc. Rev.*, 2015, **44**, 5016–5030.
165 Z. P. Smith and B. D. Freeman, *Angew. Chem., Int. Ed.*, 2014, **53**, 10286–10288.
166 C. Meng, Y. Sheng, Q. Chen, H. Tan and H. Liu, *J. Membr. Sci.*, 2017, **526**, 25–31.
167 C. Meng, Q. Chen, H. Tan, Y. Sheng and H. Liu, *J. Membr. Sci.*, 2018, **555**, 398–406.
168 F. Qie, J. Guo, B. Tu, X. Zhao, Y. Zhang and Y. Yan, *Chem. – Asian J.*, 2018, **13**, 2812–2817.
169 C. Meng, Q. Chen, X. Li and H. Liu, *J. Membr. Sci.*, 2019, **582**, 83–90.
170 C. Meng, S. Zhang, Q. Chen, X. Li and H. Liu, *ACS Appl. Mater. Interfaces*, 2020, **12**, 10893–10901.
171 W. Shi and D. L. Plata, *Green Chem.*, 2018, **20**, 5237–5406.
172 M. Xue, B. Li, S. Qiu and B. Chen, *Mater. Today*, 2016, **19**, 503–515.
173 C. Li and L. Heinke, *Symmetry*, 2020, **12**, 1–13.
174 S. Mukherjee, A. V. Desai and S. K. Ghosh, *Coord. Chem. Rev.*, 2018, **367**, 82–126.
175 S. Xie, Z. Zhang, Z. Wang and L. Yuan, *J. Am. Chem. Soc.*, 2011, **133**, 11892–11895.
176 Z. G. Gu, W. Q. Fu, X. Wu and J. Zhang, *Chem. Commun.*, 2016, **52**, 772–775.
177 P. Peluso, V. Mamane and S. Cossu, *J. Chromatogr. A*, 2014, **1363**, 11–26.

 This journal is © The Royal Society of Chemistry 2022

Open Access Article. Published on 20 May 2022. Downloaded on 14/09/2025 22:14:34.
This article is licensed under a Creative Commons Attribution-NonCommercial 3.0 Unported Licence.

178 J. Hou, H. Zhang, G. P. Simon and H. Wang, *Adv. Mater.*, 2020, **32**, 1–13.
179 J. M. Holcroft, K. J. Hartlieb, P. Z. Moghadam, J. G. Bell, G. Barin, D. P. Ferris, E. D. Bloch, M. M. Algaradah, M. S. Nassar, Y. Y. Botros, K. M. Thomas, J. R. Long, R. Q. Snurr and J. F. Stoddart, *J. Am. Chem. Soc.*, 2015, **137**, 5706–5719.
180 J. Zhang, S. Chen, A. Zingiryan and X. Bu, *J. Am. Chem. Soc.*, 2008, **130**, 17246–17247.
181 M. J. Ingleson, J. Bacsa and M. J. Rosseinsky, *Chem. Commun.*, 2007, 3036–3038.
182 R. E. Morris and X. Bu, *Nat. Chem.*, 2010, **2**, 353–361.
183 Y. Liu, W. Xuan and Y. Cui, *Adv. Mater.*, 2010, **22**, 4112–4135.
184 J. S. Seo, D. Whang, H. Lee, S. I. Jun, J. Oh, Y. J. Jeon and K. Kim, *Nature*, 2000, **404**, 982–986.
185 L. Ma, C. Abney and W. Lin, *Chem. Soc. Rev.*, 2009, **38**, 1248–1256.
186 K. J. Hartlieb, J. M. Holcroft, P. Z. Moghadam, N. A. Vermeulen, M. M. Algaradah, M. S. Nassar, Y. Y. Botros, R. Q. Snurr and J. F. Stoddart, *J. Am. Chem. Soc.*, 2016, **138**, 2292–2301.
187 P. Li, Y. He, J. Guang, L. Weng, J. C. G. Zhao, S. Xiang and B. Chen, *J. Am. Chem. Soc.*, 2014, **136**, 547–549.
188 W. Wang, X. Dong, J. Nan, W. Jin, Z. Hu, Y. Chen and J. Jiang, *Chem. Commun.*, 2012, **48**, 7022–7024.
189 Y. Lu, H. Zhang, J. Y. Chan, R. Ou, H. Zhu, M. Forsyth, E. M. Marijanovic, C. M. Doherty, P. J. Marriott, M. M. B. Holl and H. Wang, *Angew. Chem., Int. Ed.*, 2019, **58**, 16928–16935.
190 D. Dang, P. Wu, C. He, Z. Xie and C. Duan, *J. Am. Chem. Soc.*, 2010, **132**, 14321–14323.
191 F. Song, C. Wang, J. M. Falkowski, L. Ma, W. Lin, N. Carolina and U. States, *J. Am. Chem. Soc.*, 2010, **132**, 15390–15398.
192 M. Banerjee, S. Das, M. Yoon, H. J. Choi and M. H. Hyun, *J. Am. Chem. Soc.*, 2009, **131**, 7524–7525.
193 L. Ma, J. M. Falkowski, C. Abney and W. Lin, *Nat. Chem.*, 2010, **2**, 838–846.
194 C. J. Kepert, T. J. Prior and M. J. Rosseinsky, *J. Am. Chem. Soc.*, 2000, **122**, 5158–5168.
195 B. Liu, O. Shekhah, H. K. Arslan, J. Liu, C. Wöll and R. A. Fischer, *Angew. Chem., Int. Ed.*, 2012, **51**, 807–810.
196 Z. Kang, M. Xue, L. Fan, J. Ding, L. Guo, L. Gao and S. Qiu, *Chem. Commun.*, 2013, **49**, 10569–10571.
197 Z. Qiao, Z. Wang, C. Zhang, S. Yuan, Y. Zhu and J. Wang, *AIChE J.*, 2012, **59**, 4364–4372.
198 P. Brunet, M. Simard and J. D. Wuest, *J. Am. Chem. Soc.*, 1997, **119**, 2737–2738.
199 J. Zhao, H. Li, Y. Han, R. Li, X. Ding, X. Feng and B. Wang, *J. Mater. Chem. A*, 2015, **3**, 12145–12148.
200 S. Y. Zhang, L. Wojtas and M. J. Zaworotko, *J. Am. Chem. Soc.*, 2015, **137**, 12045–12049.
201 X. Hou, T. Xu, Y. Wang, S. Liu, J. Tong and B. Liu, *ACS Appl. Mater. Interfaces*, 2017, **9**, 32264–32269.
202 X. Hou, T. Xu, Y. Wang, S. Liu, J. Tong and B. Liu, *ACS Appl. Mater. Interfaces*, 2017, **9**, S1–S15.
203 X. Hou, T. Xu, Y. Wang, S. Liu, R. Chu, J. Zhang and B. Liu, *ACS Appl. Mater. Interfaces*, 2018, **10**, 26365–26371.
204 J. Y. Chan, H. Zhang, Y. Nolvachai, Y. Hu, H. Zhu, M. Forsyth, Q. Gu, D. E. Hoke, X. Zhang, P. J. Marriot and H. Wang, *Angew. Chem., Int. Ed.*, 2018, **57**, 17130–17134.
205 X. Wang, Y. Zhu, J. Liu, C. Liu, C. Cao and W. Song, *Chem. – Asian J.*, 2018, **13**, 1535–1538.
206 A. Abbas, Z. X. Wang, Z. Li, H. Jiang, Y. Liu and Y. Cui, *Inorg. Chem.*, 2018, **57**, 8697–8700.
207 Y. Peng, T. Gong and Y. Cui, *Chem. Commun.*, 2013, **49**, 8253–8255.
208 H. Wang, S. Zhao, Y. Liu, R. Yao, X. Wang, Y. Cao, D. Ma, M. Zou, A. Cao, X. Feng and B. Wang, *Nat. Commun.*, 2019, **10**, 1–9.
209 T. Rajkumar, D. Kukkar, K. Kim, J. Ryeul and A. Deep, *J. Ind. Eng. Chem.*, 2019, **72**, 50–66.
210 A. W. Peters, T. C. Wang and P. Deria, *Chem. Commun.*, 2017, **53**, 7561–7564.
211 C. Yang, Y.-Z. Zheng and X.-P. Yan, *RSC Adv.*, 2017, **7**, 36297–36301.
212 R. A. Smaldone, R. S. Forgan, H. Furukawa, J. J. Gassensmith, A. M. Z. Slawin, O. M. Yaghi and J. F. Stoddart, *Angew. Chem., Int. Ed.*, 2010, **49**, 8630–8634.
213 T. Chen, H. Tan, Q. Chen, L. Gu, Z. Wei and H. Liu, *ACS Appl. Mater. Interfaces*, 2019, **11**, 48402–48411.
214 L. Chen, X. Wang, W. Lu, X. Wu and J. Li, *Chem. Soc. Rev.*, 2016, **45**, 2137–2211.
215 D. R. Kryscio and N. A. Peppas, *Acta Biomater.*, 2012, **8**, 461–473.
216 S. Lai, S. Tang, J. Xie, C. Cai, X. Chen and C. Chen, *J. Chromatogr. A*, 2017, **1490**, 63–73.
217 W. J. Cheong, F. Ali, J. H. Choi, J. O. Lee and K. Yune Sung, *Talanta*, 2013, **106**, 45–59.
218 S. Yang, Y. Wang, Y. Jiang, S. Li and W. Liu, *Polymers*, 2016, **8**, 1–16.
219 M. Yoshikawa, K. Tharpa and S. Dima, *Chem. Rev.*, 2016, **116**, 11500–11528.
220 M. Yoshikawa, *Bioseparation*, 2001, **10**, 277–286.
221 A. S. Michaels, R. F. Baddour, H. J. Bixler and C. Y. Choo, *Ind. Eng. Chem. Process Des. Dev.*, 1962, **1**, 14–25.
222 G. Wulff, A. Sarhan and K. Zabrocki, *Tetrahedron Lett.*, 1973, **14**, 4329–4332.
223 G. Wulff and G. Kirstein, *Angew. Chem., Int. Ed. Engl.*, 1990, **29**, 684–686.
224 G. Wulff, *Angew. Chem., Int. Ed. Engl.*, 1995, **34**, 1812–1832.
225 M. Yoshikawa, J. Izumi, T. Ooi and T. Kitao, *Polym. Bull.*, 1998, **40**, 517–524.
226 Y. Kondo, M. Yoshikawa and H. Okushita, *Polym. Bull.*, 2000, **44**, 517–524.
227 M. Yoshikawa, N. Hotta, J. Kyoumura, Y. Osagawa and T. Aoki, *Sens. Actuators, B*, 2005, **104**, 282–288.
228 M. Yoshikawa, K. Murakoshi and T. Kogita, *Eur. Polym. J.*, 2006, **42**, 2532–2539.
229 M. Yoshikawa, J. Izumi and T. Kitao, *Macromolecules*, 1996, **29**, 8197–8203.

Open Access Article. Published on 20 May 2022. Downloaded on 14/09/2025 22:14:34.
This article is licensed under a Creative Commons Attribution-NonCommercial 3.0 Unported Licence.

230 M. Yoshikawa, T. Fujisawa, J. Izumi, T. Kitao and S. Sakamoto, *Anal. Chim. Acta*, 1998, **365**, 59–67.
231 M. Yoshikawa, T. Fujisawa and J. Izumi, *Macromol. Chem. Phys.*, 1999, **365**, 1458–1465.
232 M. Yoshikawa, J. Izumi and T. Kitao, *React. Funct. Polym.*, 1999, **42**, 93–102.
233 M. Yoshikawa, A. Shimada and J. Izumi, *Analyst*, 2001, **126**, 775–780.
234 M. Yoshikawa, J. Izumi, T. Kitao and S. Koya, *J. Membr. Sci.*, 1995, **108**, 171–175.
235 M. Yoshikawa, K. Koso, K. Yonetani, S. Kitamura and S. Kimura, *J. Polym. Sci., Part A: Polym. Chem.*, 2005, **43**, 385–396.
236 M. Yoshikawa, J. Izumi and T. Kitao, *Chem. Lett.*, 1996, **25**, 611–612.
237 Y. Kondo, Y. Morita, A. Fujimoto, M. Tounai, S. Kimura and M. Yoshikawa, *Chirality*, 2003, **14**, 498–503.
238 J. Izumi, M. Yoshikawa and T. Kitao, *Maku*, 1997, **22**, 149–154.
239 M. Hatanaka, Y. Nishioka and M. Yoshikawa, *J. Appl. Polym. Sci.*, 2013, **128**, 123–131.
240 M. Hatanaka, Y. Nishioka and M. Yoshikawa, *J. Membr. Sep. Technol.*, 2013, **2**, 109–119.
241 M. Hatanaka, Y. Nishioka and M. Yoshikawa, *J. Mater. Sci. Res.*, 2012, **1**, 114–122.
242 M. Hatanaka, Y. Nishioka and M. Yoshikawa, *Macromol. Chem. Phys.*, 2011, **212**, 1351–1359.
243 Y. Sueyoshi, C. Fukushima and M. Yoshikawa, *J. Membr. Sci.*, 2010, **357**, 90–97.
244 M. Yoshikawa, T. Ooi and J. Izumi, *J. Appl. Polym. Sci.*, 1999, **72**, 493–499.
245 Y. Sueyoshi, A. Utsunomiya, M. Yoshikawa, G. P. Robertson and M. D. Guiver, *J. Membr. Sci.*, 2012, **401–402**, 89–96.
246 M. Yoshikawa, J. Izumi and T. Kitao, *Polym. J.*, 1997, **29**, 205–210.
247 A. Dzgoev and K. Haupt, *Chirality*, 1999, **11**, 465–469.
248 P. Screenivasulu Reddy, T. Kobayashi, M. Abe and N. Fujii, *Eur. Polym. J.*, 2002, **38**, 521–529.
249 Z. Jiang, Y. Yu and H. Wu, *J. Membr. Sci.*, 2006, **280**, 876–882.
250 S. Son and J. Jegal, *J. Appl. Polym. Sci.*, 2006, **104**, 1866–1872.
251 N. Bing, Z. Xu, X. Wang, Z. Yang and H. Yang, *J. Appl. Polym. Sci.*, 2007, **106**, 71–76.
252 Y. Lei, F. Chen and Y. Luo, *Iran. Polym. J.*, 2014, **23**, 679–687.
253 B. Gao, Y. Li and K. Cui, *Int. J. Polym. Mater. Polym. Biomater.*, 2018, **67**, 517–527.
254 H. Li, Q. Huang, D. Li, S. Li, X. Wu, L. Wen and C. Ban, *Org. Process Res. Dev.*, 2018, **22**, 278–285.
255 T. Masawaki, M. Sasai and S. Tone, *J. Chem. Eng. Jpn.*, 1992, **25**, 33–39.
256 R. Viveiros, S. Rebocho and T. Casimiro, *Polymer*, 2018, **10**, 1–27.
257 L. Madikizela, S. Ncube and L. Chimuka, in *Mip Synthesis, Characteristics and Analytical Application*, Elsevier B.V., 1st edn, 2019, vol. 86, pp. 337–364.
258 R. A. Lorenzo, A. M. Carro, C. Alvarez-lorenzo and A. Concheiro, *Int. J. Mol. Sci.*, 2011, **12**, 4327–4347.
259 E. Drioli, A. Brunetti, G. Di Profio and G. Barbieri, *Green Chem.*, 2012, **14**, 1561–1572.
260 S. H. Park, A. Alammar, Z. Fulop, B. A. Pulido, S. P. Nunes and G. Szekely, *Green Chem.*, 2021, **23**, 1175–1184.
261 W. Xie, T. Li, A. Tiraferri, E. Drioli, A. Figoli, J. C. Crittenden and B. Liu, *ACS Sustainable Chem. Eng.*, 2021, **9**, 50–75.
262 W. J. Lee, P. S. Goh, W. J. Lau, A. F. Ismail and N. Hilal, *Membranes*, 2021, **11**, 1–35.
263 J. W. Lee, *Ind. Eng. Chem. Res.*, 2020, **59**, 9619–9628.
264 X. Lin, R. Gong, J. Li, P. Li, J. Yu and A. E. Rodrigues, *J. Chromatogr. A*, 2016, **1467**, 347–355.
265 D. Antos and A. Seidel-Morgenstern, *Chem. Eng. Sci.*, 2001, **56**, 6667–6682.
266 D. B. Broughton and C. G. Gerhold, US2985589, 1961.
267 M. Negawa and F. Shoji, *J. Chromatogr. A*, 1992, **590**, 113–117.
268 T. Futagawa, J. P. Canvant, E. Cavoy, M. Deleers, M. Hamende and V. Zimmermann, US6107492, 2000.
269 H. A. Zinnen and M. J. Gattuso, US6455736, 2002.
270 M. J. Gattuso, US5889186, 1999.
271 H. A. Zinnen and M. J. Gattuso, US6410794, 2002.
272 A. L. L. Duchateau, R. Gebhard and Q. B. Broxterman, WO2006/0122430, 2006.
273 H. Diehl, A. Krebs, E. Krebs, W. Lange, H. Paul, D. Seidel, R. Grosser and T. Reichelt, US7709644B2, 2010.
274 C. B. Ching, B. G. Lim, E. J. D. Lee and S. C. Ng, *J. Chromatogr.*, 1993, **634**, 215–219.
275 B. Lim, C. Ching, R. B. H. Tan and S. C. Ng, *Chem. Eng. Sci.*, 1995, **50**, 2289–2298.
276 B. G. Lim and C. B. Ching, *J. Chromatogr. A*, 1996, **734**, 247–258.
277 A. S. Andrade Neto, A. R. Secchi, M. B. Souza Jr. and A. G. Barreto Jr., *J. Chromatogr. A*, 2016, **1470**, 42–49.
278 F. C. Cunha, A. R. Secchi, M. B. de Souza and A. G. Barreto, *Chirality*, 2019, **31**, 583–591.
279 O. Ludemann-Hombourger, R. M. Nicoud and M. Bailly, *Sep. Sci. Technol.*, 2000, **35**, 1829–1862.
280 L. S. Pais, J. M. Loureiro and A. E. Rodrigues, *AIChE J.*, 1998, **44**, 561–569.
281 Z. Zhang, M. Mazzotti and M. Morbidelli, *Korean J. Chem. Eng.*, 2004, **21**, 454–464.
282 I. B. R. Nogueira, A. M. Ribeiro, R. Requião, K. V. Pontes, H. Koivisto, A. E. Rodrigues and J. M. Loureiro, *Appl. Soft Comput. J.*, 2018, **67**, 29–47.
283 P. Suvarov, J. W. Lee, A. Vande Wouwer, A. Seidel-Morgenstern and A. Kienle, *J. Chromatogr. A*, 2019, **1602**, 266–272.
284 J. Matos, R. P. V. Faria, I. B. R. Nogueira, J. M. Loureiro and A. M. Ribeiro, *Comput. Chem. Eng.*, 2019, **123**, 344–356.

 This journal is © The Royal Society of Chemistry 2022

Open Access Article. Published on 20 May 2022. Downloaded on 14/09/2025 22:14:34.
This article is licensed under a Creative Commons Attribution-NonCommercial 3.0 Unported Licence.

285 C. Migliorini, M. Wendlinger, M. Mazzotti and M. Morbidelli, *Ind. Eng. Chem. Res.*, 2001, **40**, 2606–2617.
286 S. Abel, M. Mazzotti and M. Morbidelli, *J. Chromatogr. A*, 2002, **944**, 23–39.
287 J. Houwing, T. B. Jensen, S. H. Van Hateren, H. A. H. Billiet and L. A. M. Van der Wielen, *AIChE J.*, 2003, **49**, 665–674.
288 T. B. Jensen, T. G. P. Reijns, H. A. H. Billiet and L. A. M. van der Wielen, *J. Chromatogr. A*, 2000, **873**, 149–162.
289 M. M. Kearney and K. L. Hieb, US5102553, 1992.
290 H. Schramm, M. Kaspereit, A. Kienle and A. Seidel-Morgenstern, *Chem. Eng. Technol.*, 2002, **25**, 1151–1155.
291 R. C. Vroon, M. A. Boon and P. J. T. Bussman, WO2015/0314218, 2015.
292 M. Anton, WO2017/199031, 2017.
293 T. H. Yoon, B. H. Chung and I. H. Kim, *Biotechnol. Bioprocess Eng.*, 2004, **9**, 285–291.
294 K. B. Lee, C. Y. Chin, Y. Xie, G. B. Cox and N. H. L. Wang, *Ind. Eng. Chem. Res.*, 2005, **44**, 3249–3267.
295 K. B. Lee, S. Mun, F. Cauley, G. B. Cox and N. H. L. Wang, *Ind. Eng. Chem. Res.*, 2006, **45**, 739–752.
296 Y. Zhang, K. Hidajat and A. K. Ray, *Chem. Eng. Sci.*, 2007, **62**, 1364–1375.
297 J. S. Park, W. S. Kim, J. M. Kim and I. H. Kim, *J. Chem. Eng. Jpn.*, 2008, **41**, 624–626.
298 P. S. Gomes, M. Zabkova, M. Zabka, M. Minceva and A. E. Rodrigues, *AIChE J.*, 2009, **56**, 125–142.
299 A. E. Ribeiro, P. S. Gomes, L. S. Pais and A. E. Rodrigues, *Sep. Sci. Technol.*, 2011, **46**, 1726–1739.
300 R. S. Arafah, A. E. Ribeiro, A. E. Rodrigues and L. S. Pais, *Chirality*, 2019, **31**, 62–71.
301 R. Gong, X. Lin, P. Li, J. Yu and A. E. Rodrigues, *J. Chromatogr. A*, 2014, **1363**, 242–249.
302 Y. Yang, K. Lu, R. Gong, D. Qu, P. Li, J. Yu and A. E. Rodrigues, *Adsorption*, 2019, **25**, 1227–1240.
303 C. G. Lee, Y. J. Song, K. B. Lee and S. Mun, *J. Ind. Eng. Chem.*, 2019, **80**, 677–685.
304 C. G. Lee, C. Y. Jo, K. B. Lee and S. Mun, *Sep. Purif. Technol.*, 2021, **254**, 117597.
305 A. E. Ribeiro, N. S. Graça, L. S. Pais and A. E. Rodrigues, *Sep. Purif. Technol.*, 2008, **61**, 375–383.
306 X. Jiang, L. Zhu, B. Yu, Q. Su, J. Xu and W. Yu, *J. Chromatogr. A*, 2018, **1531**, 131–142.
307 M. Fuereder, C. Femmer, G. Storti, S. Panke and M. Bechtold, *Chem. Eng. Sci.*, 2016, **152**, 649–662.
308 I. Harriehausen, K. Wrzosek, H. Lorenz and A. Seidel-Morgenstern, *Adsorption*, 2020, **26**, 1199–1213.
309 M. Johannsen and G. Brunner, *J. Supercrit. Fluids*, 2018, **134**, 61–70.
310 S. Peper, M. Lübbert, M. Johannsen and G. Brunner, *Sep. Sci. Technol.*, 2002, **37**, 2545–2566.
311 D. Speybrouck and E. Lipka, *J. Chromatogr. A*, 2016, **1467**, 33–55.
312 C. J. Welch, W. R. Leonard, J. O. DaSilva, M. Biba, J. Albaneze-Walker, D. W. Henderson, B. Laing and D. J. Mathre, *LC-GC Asia Pac.*, 2005, **18**, 24–31.
313 L. Miller, *J. Chromatogr. A*, 2012, **1250**, 250–255.
314 K. Kalíková, T. Šlechtová, J. Vozka and E. Tesařová, *Anal. Chim. Acta*, 2014, **821**, 1–33.
315 A. Ghinet, Y. Zehani and E. Lipka, *J. Pharm. Biomed. Anal.*, 2017, **145**, 845–853.
316 E. R. Francotte, *Practical Aspects and Applications of Preparative Supercritical Fluid Chromatography*, Elsevier Inc., 2017.
317 S. H. Yip, D. Wu, J. Kempson, A. Hernandez, H. Zhang, P. Li, D. Sun and A. Mathur, *Sep. Sci. Plus*, 2019, **2**, 343–352.
318 C. West, *TrAC, Trends Anal. Chem.*, 2019, **120**, 1–9.
319 D. Speybrouck, M. Howsam and E. Lipka, *Trends Anal. Chem.*, 2020, **133**, 1–16.
320 R. M. Nicoud, *Ind. Eng. Chem. Res.*, 2014, **53**, 3755–3765.
321 J. Y. Clavier, R. M. Nicoud and M. Perrut, *Process Technol. Proc.*, 1996, **12**, 429–434.
322 M. Mazzotti, G. Storti and M. Morbidelli, *J. Chromatogr. A*, 1997, **786**, 309–320.
323 F. Denet, W. Hauck, R. M. Nicoud, O. Di Giovanni, M. Mazzotti, J. N. Jaubert and M. Morbidelli, *Ind. Eng. Chem. Res.*, 2001, **40**, 4603–4609.
324 S. Peper, M. Johannsen and G. Brunner, *J. Chromatogr. A*, 2007, **1176**, 246–253.
325 M. Johannsen, S. Peper and A. Depta, *J. Biochem. Biophys. Methods*, 2002, **54**, 85–102.
326 A. Rajendran, S. Peper, M. Johannsen, M. Mazzotti, M. Morbidelli and G. Brunner, *J. Chromatogr. A*, 2005, **1092**, 55–64.
327 H. Kaemmerer, G. Brunner and M. Johannsen, *J. Supercrit. Fluids*, 2007, **43**, 204–213.
328 M. A. Korany, H. Mahgoub, R. S. Haggag, M. A. A. Ragab and O. A. Elmallah, *J. Liq. Chromatogr. Relat. Technol.*, 2017, **40**, 839–852.
329 H. R. Hobbs, B. Kondor, P. Stephenson, R. A. Sheldon, N. R. Thomas and M. Poliakoff, *Green Chem.*, 2006, **8**, 816–821.
330 T. Matsuda, T. Harada and K. Nakamura, *Green Chem.*, 2004, **6**, 440–444.
331 M. T. Reetz, W. Wiesenhöfer, G. Franciò and W. Leitner, *Adv. Synth. Catal.*, 2003, **345**, 1221–1228.
332 T. Matsuda, K. Watanabe, T. Harada, K. Nakamura, Y. Arita, Y. Misumi, S. Ichikawa and T. Ikariya, *Chem. Commun.*, 2004, 2286–2287.
333 P. Lozano, T. De Diego, C. Mira, K. Montague, M. Vaultier and J. L. Iborra, *Green Chem.*, 2009, **11**, 538–554.
334 Z. Molnár, E. Farkas, Á. Lakó, B. Erdélyi, W. Kroutil, B. G. Vértessy, C. Paizs and L. Poppe, *Catalysts*, 2019, **9**, 1–11.
335 S. Mane, *Anal. Methods*, 2016, **8**, 7567–7586.
336 B. Schuur, B. J. V. Verkuijl, A. J. Minnaard, J. G. De Vries, H. J. Heeres and B. L. Feringa, *Org. Biomol. Chem.*, 2011, **9**, 36–51.
337 B. Schuur, J. G. M. Winkelman, J. G. de Vries and H. J. Heeres, *Chem. Eng. Sci.*, 2010, **65**, 4682–4690.

Open Access Article. Published on 20 May 2022. Downloaded on 14/09/2025 22:14:34.
This article is licensed under a Creative Commons Attribution-NonCommercial 3.0 Unported Licence.

338 A. Holbach, J. Godde, R. Mahendrarajah and N. Kockmann, *AIChE J.*, 2015, **61**, 266–276.
339 K. Tang, P. Wen, P. Zhang and Y. Huang, *Sep. Purif. Technol.*, 2014, **134**, 100–109.
340 B. Schuur, A. J. Hallett, J. G. M. Winkelman, J. G. De Vries and H. J. Heeres, *Org. Process Res. Dev.*, 2009, **13**, 911–914.
341 K. Tang, P. Wen, P. Zhang and Y. Huang, *Chirality*, 2015, **27**, 75–81.
342 K. Tang, H. Zhang and P. Zhang, *Ind. Eng. Chem. Res.*, 2013, **52**, 3893–3902.
343 K. Tang, H. Zhang and Y. Liu, *AIChE J.*, 2013, **59**, 2594–2602.
344 D. J. C. Constable, P. J. Dunn, J. D. Hayler, G. R. Humphrey, J. L. Leazer, R. J. Linderman, K. Lorenz, J. Manley, B. A. Pearlman, A. Wells, A. Zaks and T. Y. Zhang, *Green Chem.*, 2007, **9**, 411–420.
345 A. Jordan, P. Stoy and H. F. Sneddon, *Chem. Rev.*, 2021, **121**, 1582–1622.
346 N. Rubio and C. Minguillón, in *Chiral Recognition in Separation Methods: Mechanisms and Applications*, 2010, pp. 241–274.
347 G. K. E. Scriba, *Chiral Separations - Methods and Protocols*, Humana Press, 3rd edn, 2019.
348 A. P. Foucault, *J. Chromatogr. A*, 2001, **906**, 365–378.
349 A. Berthod, M. J. Ruiz-Ángel and S. Carda-Broch, *J. Chromatogr. A*, 2009, **1216**, 4206–4217.
350 X. Y. Huang, D. Pei, J. F. Liu and D. L. Di, *J. Chromatogr. A*, 2018, **1531**, 1–12.
351 X. Y. Huang and D. L. Di, *TrAC, Trends Anal. Chem.*, 2015, **67**, 128–133.
352 A. E. Kostanyan and A. A. Erastov, *J. Chromatogr. A*, 2015, **1406**, 118–128.
353 N. Rubio, S. Ignatova, C. Minguillón and I. A. Sutherland, *J. Chromatogr. A*, 2009, **1216**, 8505–8511.
354 P. Zhang, G. Sun, K. Tang, C. Zhou, C. Yang and W. Yang, *Sep. Purif. Technol.*, 2015, **146**, 276–283.
355 P. Zhang, G. Sun, K. Tang, W. Yang, G. Sui and C. Zhou, *J. Sep. Sci.*, 2014, 1–8.
356 S. Tong, Y. Guan, J. Yan, B. Zheng and L. Zhao, *J. Chromatogr. A*, 2011, **1218**, 5434–5440.
357 F. Couillard, A. Foucault and D. Durand, US7422685B2, 2008.
358 I. Sutherland, P. Hewitson and S. Ignatova, *J. Chromatogr. A*, 2009, **1216**, 8787–8792.

 This journal is © The Royal Society of Chemistry 2022